

1
2
3
4
5
6
7
8
9
10
11
12
13
14
15
16
17
18
19
20
21
22
23
24
25
26
27
28
29
30
31
32

Intraspecific variation in the duration of epigenetic inheritance

François Frejacques^{1,6}, Marie Saglio^{1,3,6}, Mohammed Aljohani^{1,2,5}, Christian Froekjaer-Jensen², Lise Frézal^{1,4,7}, and Marie-Anne Félix^{1,7}

1: IBENS, Department of Biology, Ecole Normale Supérieure, CNRS, Inserm, PSL Research University, Paris, France

2: Bioscience Program, Biological and Environmental Science and Engineering (BESE), King Abdullah University of Science and Technology (KAUST), Thuwal, 23955-6900, Kingdom of Saudi Arabia

3: Present address: Department of Developmental and Stem Cell Biology, Institut Pasteur, Paris, France

4: Present address: Institut Pasteur, Université Paris Cité, Unité des Bactéries pathogènes entériques, Paris, France

5: Present address: Department of Genome Sciences, University of Washington, Seattle, WA 98195, USA

6: First authors, alphabetical order

7: Correspondence: lise.frezal@pasteur.fr, felix@bio.ens.psl.eu (lead contact)

33 **Abstract**

34

35 Epigenetic inheritance is generally less stable across generations than DNA sequence-based
36 heredity. One common form of epigenetic inheritance, found in plants, fungi, and animals, is
37 the transgenerational memory of gene silencing mediated by small RNAs. These small RNAs
38 can be amplified through RNA-dependent RNA polymerases, thus maintaining the silenced
39 state across multiple generations. Such molecular mechanisms raise questions regarding
40 their natural variation and evolutionary impact. We here ask whether the presence and
41 duration of epigenetic inheritance display genetic variation within a species. We use the
42 ability of the nematode *Caenorhabditis elegans* to silence genes for multiple generations
43 after an initial RNA interference trigger. We find that the presence and the duration of
44 silencing in number of generations differ across *C. elegans* wild strains. Strikingly, several
45 wild strains show no memory, while some display a longer memory than the reference
46 strain. Natural DNA sequence polymorphisms, such as in the *set-24* and *drh-1* genes, affect
47 epigenetic memory of an external trigger, demonstrating that intraspecific DNA sequence
48 evolution affects the duration of epigenetic inheritance. We further show that the duration
49 of silencing memory in wild strains is quite robust to environmental variation such as diet
50 and passage through larval diapauses, but not to temperature variation. Altogether, these
51 results demonstrate intraspecific diversity in the regulation of small RNA-based heredity, a
52 prerequisite for selection acting on genetic variants affecting epigenetic inheritance
53 duration.

54

55

56

57

58 Keywords: epigenetic inheritance, evolution, *C. elegans*, small RNAs

59 Introduction

60

61 Various molecular mechanisms of epigenetic inheritance have been uncovered over the last
62 decade across biological kingdoms, thus renewing the interest about the importance of such
63 non-conventional inheritance in evolution (Lind and Spagopoulou, 2018; Bonduriansky and
64 Day, 2018; Adrian-Kalchhauser et al., 2020; Duempelmann, Skribbe et al., 2020; Ashe et al.,
65 2021). Two features distinguish epigenetic variation from DNA sequence variation: 1)
66 epigenetic variants may originate not only stochastically but also through environmental
67 induction; 2) epigenetic variants are generally less stable over generations than DNA
68 sequence. We here focus on this latter point, regarding the stability of epigenetic variants
69 across generations. At a large macroevolutionary scale, this duration ranges from long-term
70 stability of methylated epialleles in plants (Cubas et al., 1999; Weigel and Colot, 2012; Miska
71 and Ferguson-Smith, 2016; Fitz-James and Cavalli, 2022) or of paramutation in *Drosophila*
72 (de Vanssay et al., 2012) to a lack of clear demonstration of a multigenerational memory in
73 mammals beyond parental or grandparental effects (Heard and Martienssen, 2014). In the
74 midst of this stability spectrum lies small RNA silencing in the nematode *Caenorhabditis*
75 *elegans*, with a few generations of memory of the initial trigger in a commonly used
76 experimental paradigm. This intermediate range of a few generations offers a particularly
77 favorable case to study its variation within the species and the possible evolutionary
78 significance of this variation.

79 Specifically, the *C. elegans* reference strain N2 is able to transmit the memory of
80 silencing by double-stranded RNA, for example after an initial trigger of exogenous RNA
81 interference (RNAi). The primary small RNAs are amplified in secondary small RNAs by RNA-
82 dependent RNA polymerases (Sijen, Fleenor, Simmer et al., 2001; and Fire, 2007; Vasale, W.
83 Gu et al., 2010; Pak et al., 2012; Tsai et al., 2015; X. Chen, K. Wang, Mufti et al., 2024). This
84 amplification in principle can maintain the memory of the initial signal over several
85 generations even after it has been removed (Gu et al., 2012; Billi et al., 2014; F. Xu, X. Feng
86 et al., 2018; Shukla et al., 2021; Ouyang et al., 2022). Many factors required for the
87 inheritance of small RNA pools were discovered using laboratory genetic screens in the N2
88 reference background (e.g. Grishok et al., 2000; Vastenhouw et al., 2006; Buckley, Burkhart
89 et al., 2012; Lev, Seroussi et al. 2017; Spracklin et al., 2017; Du, Shi et al., 2023; Chen and
90 Phillips, 2024). The RNAi memory mechanism is distinct from the RNAi mechanism itself
91 (Grishok et al., 2000; Buckley, Burkhart et al., 2012).

92 This molecular mechanism of amplification and inheritance along generations raises
93 questions regarding its ecological and evolutionary context. A prerequisite for studying how
94 natural selection may act on epigenetic inheritance duration is to detect intraspecific
95 diversity in the initiation and duration of epigenetic inheritance. The aim of the present work
96 is to measure intraspecies variation for RNAi memory duration in *C. elegans*. Note, that we
97 will not explore the natural variation in epialleles (here small RNA sequence representation),
98 nor which external ecological factors may trigger initial variation in small RNA pools (Baugh
99 and Day, 2020), but how long the memory of such triggers remains.

100 We probe natural strains of *C. elegans* for their transmission of an initial RNAi trigger
101 and find that they differ in both occurrence and duration of their RNAi memory. We show
102 that natural DNA sequence polymorphisms in the *set-24*, *drh-1* and *eri-6/7* genes may affect
103 epigenetic memory of silencing. In addition to genetic variation, we find that the RNAi
104 memory duration varies with temperature and is quite insensitive to our other tested
105 environments, including starvation, passage through dauer diapause or bacterial diet. More

106 importantly, the detection of intraspecific genetic variation for the presence and duration of
107 RNAi memory means that, like any quantitative trait, epigenetic inheritance can respond to
108 standard natural selection.

109 Results

110

111 The duration of RNAi silencing memory varies among *C. elegans* wild isolates

112 We first selected genetically divergent *C. elegans* wild isolates that are sensitive to RNAi.
113 Based on the data by (Paaby et al., 2015; Crombie et al., 2019) and our prior work with the
114 MY10 strain (Frézal et al., 2018), we focused on the eight wild strains shown in Fig. 1A. We
115 used two distinct transgenes to assay small RNA silencing and two methods to introduce
116 them into wild genetic backgrounds. First, we introduced a single-copy *pie-*
117 *1p::GFP::H2B::pie-1* transgene by repeated backcrosses to the target wild isolate background
118 (Ashe, Sapetschnig et al., 2012). With this transgene, fluorescence is restricted to the
119 germline nuclei and strictly nuclear because of the histone protein fusion (Fig. 1B). Second,
120 we used CRISPR/Cas9 genome editing to introduce at the same site in all wild isolate
121 backgrounds a specifically engineered *mex-5p::ce-GFP::tbb-2* transgene, optimized for high
122 expression and devoid of piRNA sites (Aljohani et al., 2020). As a result, the germline-specific
123 localization of this *C. elegans* enhanced GFP (*ce-gfp*) is brighter, and fluorescence also
124 present in the cytoplasm because, despite the nuclear localization signals, the protein is less
125 retained in the nucleus than with the histone fusion (Fig. 1B).

126 Using the protocol from (Ashe, Sapetschnig et al., 2012; Lev, Seroussi et al., 2017)
127 (Fig. 1C), we assayed the duration of RNAi memory in the reference N2 background in
128 parallel with the *pie-1p::GFP* and *mex-5p::ce-GFP* transgenes. After RNAi initiation, both
129 transgenes were initially silenced in all animals (Fig. S1A). Once the RNAi trigger was
130 removed, full silencing was maintained in the progeny (generation G1). Starting at the third
131 generation, a fraction of the population re-expressed GFP and this percentage increased
132 through generations. The two transgenes showed similar dynamics; however as can be
133 expected from the lack of piRNA sites, the RNAi memory was maintained for a shorter time
134 with the *mex-5p::ce-GFP* transgene (Fig. S1C). We further mainly used the *mex-5p::ce-GFP*
135 transgene but report below on the convergent results using both methods.

136 Our first aim was to test whether wild genetic backgrounds differed in their RNAi
137 memory duration. After a two-generation exposure to *gfp* RNAi from *E. coli* HT115 bacteria,
138 we found that the *mex-5p::ce-GFP* transgene was fully silenced in all isolates, with the
139 exception of some individuals of the MY10 strain, and that the duration of RNAi memory
140 greatly varied among wild genetic backgrounds (Fig. 1D-E, Table S2, Table S3). Once the RNAi
141 trigger was removed, a fraction of the population in the N2 reference re-expressed GFP at
142 the first generation and this percentage increased until fluorescence was fully recovered in
143 all individuals at the third or fourth generation. Some wild isolates, such as MY10, JU1171 or
144 QX1791, did not, or hardly, transmit parental GFP silencing to the first generation. Other
145 isolates, such as JU1395 or XZ1514, displayed an increased duration of RNAi memory
146 compared to N2. The results were consistent across three replicates per experiment and
147 four distinct experiments, which we call "blocks", lettered C, D, E and F (Fig. 1D, Table S2).
148 We plotted in Fig. 1E estimated half-lives of GFP silencing memory. Using this estimate, we
149 found significant differences for GFP desilencing dynamics across wild genetic backgrounds
150 (generalized linear mixed model or glmm, $p < 2 \times 10^{-16}$).

151 We further asked whether the variation among isolates could be reproduced using
152 the *pie-1p::GFP* transgene. As expected, given the possible silencing by piRNAs of the *pie-*
153 *1p::GFP::H2B::pie-1* transgene, all displayed increased RNAi memory with this transgene
154 compared to its *mex-5p::ce-GFP::tbb-2* counterpart (Fig. S1D-E). Most importantly, the

155 relative rank of RNAi memory duration of the tested wild isolates was well conserved (Fig.
156 S1D), showing that they differ in the duration of their RNAi silencing memory.

157

158 **The *set-24* DNA sequence polymorphism affects RNAi memory**

159 We then aimed to determine whether DNA sequence polymorphisms could explain variation
160 in RNAi memory, thus ruling out other types of hereditary variation that may influence this
161 phenotype. For this, we leveraged our prior knowledge of natural variation in another
162 multigenerational phenotype. The mortal germline phenotype (Mrt) is a multigenerational
163 sterility process whereby lines become sterile after several generations (Ahmed and
164 Hodgkin, 2000). Several mutations affecting small RNA pathways, chromatin remodeling and
165 RNAi memory cause a temperature-sensitive sterility phenotype in the N2 background
166 (Ahmed and Hodgkin, 2000; Buckley, Burkhart et al., 2012; Lev, Seroussi et al., 2017;
167 Spracklin et al., 2017). Interestingly, some wild isolates cultured in laboratory conditions also
168 display multigenerational sterility, which is counteracted by association with natural bacteria
169 (Frézal et al., 2018; Frézal, Saglio et al. 2023). An example is the MY10 strain, which becomes
170 sterile after only two to three generations at 25°C. (Frézal et al., 2018) showed that a partial
171 deletion of the *set-24* gene in MY10 (Fig. 2C) was a major effect variant causing a Mrt
172 phenotype. *set-24* encodes a SET-domain protein likely binding modified histones. Given the
173 relationship between RNAi memory and the Mrt phenotype, and the lack of RNAi memory of
174 the MY10 background (Fig. 1D-E), we asked whether this *set-24* polymorphism (Fig. 2C)
175 affected RNAi memory.

176 For this, we engineered in the N2 background the *set-24(bab562)* allele that mimics
177 the natural deletion from the MY10 isolate (called *set-24(mfP23)*) and crossed it to the *mex-*
178 *5p::ce-GFP::tbb-2* transgene. We found that the *set-24(bab562)* allele significantly reduced
179 RNAi memory compared to the N2 genetic background (Fig. 2A-B). This *set-24* polymorphism
180 explained only part of the difference in RNAi memory between the N2 and MY10
181 backgrounds, suggesting that further polymorphisms may underlie some RNAi memory
182 difference between the two strains. Altogether, this result demonstrates that DNA sequence
183 evolution affects epigenetic memory.

184

185 **The intermediate frequency *drh-1* polymorphism affects RNAi memory**

186 Given that the derived *set-24* deletion allele is rare in the wild (Frézal et al., 2018), we
187 wondered whether more common and thus potentially more evolutionary stable
188 polymorphisms could underlie natural variation in the duration of RNAi memory. *C. elegans*
189 antiviral defense mechanisms rely in part on recognition of viral double-stranded RNA
190 (dsRNA) and production of small RNAs targeting the virus (Ashe, BÉlicard, Le Pen, Sarkies et
191 al., 2013; Coffman et al., 2017; Sowa et al., 2020; Batachari et al., 2024). As the machinery
192 required to recognize and initiate antiviral response is in part the same as that of RNAi
193 (Tabara et al., 2002; Consalvo et al., 2024), we wondered whether polymorphisms found in
194 the double-stranded RNA antiviral pathway could also affect RNAi memory.

195 One gene involved in the complex responsible for foreign dsRNA recognition and
196 degradation is *drh-1*, a RIG-I like DExD/H box helicase with dsRNA binding activity (Duchaine
197 et al., 2006; Batachari et al., 2024; Consalvo et al., 2024). Studying variation in the sensitivity
198 to Orsay virus infection among wild *C. elegans* strains, we previously found that a 159 bp
199 natural deletion allele (*niDf250*) in the RIG-I like domain of DRH-1 was causally associated
200 with hypersensitivity to viral infection and was present at an intermediate frequency in the
201 species (Ashe, BÉlicard, Le Pen, Sarkies et al., 2013) (Fig. 3A).

202 To test whether this *drh-1* allele affected RNAi memory, we reproduced this natural
203 deletion by genome editing of the N2 genetic background, yielding allele *drh-1(bab552)*, and
204 crossed it to the *mex-5p::ce-GFP::tbb-2* transgene. The RNAi efficacy was tested in this line
205 along with the N2 and MY10 backgrounds, the latter a natural carrier of the deletion. We
206 first observed that initiating RNAi using *E. coli* iOP50 transformed with pFF1 (see Methods)
207 increased RNAi efficiency as even MY10 was almost fully silenced at G0 (Fig. 3B, Fig. S4). We
208 also noted that, when placed in an N2 background, the partial deletion of *drh-1* not only
209 reduced *gfp* RNAi memory but made animals somewhat less responsive to RNAi initiation
210 (Fig. 3B-C). The *drh-1* deletion allele is maintained at intermediate frequency in the *C.*
211 *elegans* species, particularly in Eurasia and Africa and is thus a common allele potentially
212 affecting RNAi memory (and marginally, efficiency) in natural populations.

213

214 **Structural polymorphisms at the *eri-6/7* locus likely affect RNAi memory**

215 Besides exogenous double-stranded RNAs, different endogenous small RNA pathways exist
216 in *C. elegans*. In both cases, the primary small RNAs are amplified in secondary 22G small
217 RNAs (Billi et al., 2014). Because factors required for the amplification of exogenous and
218 endogenous small RNAs are shared, the different small RNA pools compete amongst each
219 other for amplification (Houri-Ze'evi et al., 2016; Shukla et al., 2021; Karin et al., 2023). For
220 instance, the endogenous piRNA pathway modulates the duration of exogenous RNAi
221 memory: the inactivation of the piRNA pathway results in a longer exogenous RNAi memory
222 (Shukla et al., 2021). Inactivating mutations in the ERGO-1 26G-RNA pathway enhance RNAi
223 (Eri phenotype) (Kennedy et al., 2004; Lee et al., 2006; Fischer, Butler et al., 2008) but a
224 potential effect on RNAi memory had not been tested.

225 The *eri-6/7* locus produces a helicase involved in the endogenous ERGO-1 26G-RNA
226 pathway repressing retrotransposons and novel genes (Fischer et al., 2011; Fischer and
227 Ruvkun, 2020). The gene has been shown to greatly vary in structure among *C. elegans* wild
228 isolates (Fig. 4C), with an inversion of the *eri-6* part of the gene and further indels, impacting
229 the splicing efficiency of the inverted *eri-6* exons to the remaining *eri-7* exons and the
230 expression of their downstream targets (Fischer, Butler et al., 2008; G. Zhang et al., 2024).

231 We tested whether the laboratory-induced *eri-6(mg379)* splice site mutation (Fig. 4B)
232 affected the duration of exogenous RNAi silencing memory. We found that this reduction-of-
233 function mutation increased RNAi memory (Fig. 4A), possibly through the competition
234 between small RNA pools for amplification. The natural rearrangements impacting the *eri-*
235 *6/7* locus activity thus likely affect RNAi memory in *C. elegans*.

236

237 **Environmental effects on RNAi memory of *C. elegans* wild isolates**

238 Having demonstrated a genetic component in the duration of GFP silencing, we investigated
239 whether the environment may impact this duration. In natural contexts, *C. elegans* follows a
240 boom-and-bust life cycle (Fig. 5A) and is subject to multiple biotic and abiotic constraints
241 (Félix and Duveau, 2012; Frézal and Félix, 2015; Schulenburg and Félix, 2017). We focused on
242 some of these relevant factors to assess their potential impact on RNAi memory:
243 temperature, passage through diapause states (Fig. 5B-G), and bacterial environment (Fig.
244 S2A). In order to keep RNAi efficiency constant across environmental conditions, we initiated
245 GFP silencing memory as above until G0 and modified the conditions in which the
246 subsequent generations were cultured.

247 We first compared RNAi memory at two temperatures, 20°C (temperature of
248 previous assays) and 25°C, on two strains displaying different memory durations. We found

249 that the JU1395 background strain transmitted GFP silencing for a higher number of
250 generations at 25°C than at 20°C, whereas the higher temperature did not rescue the lack of
251 memory of the JU1171 strain (Fig. 5B-C). Development occurs faster at 25°C compared to
252 20°C, therefore we tested whether the longer memory in number of generations
253 corresponded to a similar memory in absolute time. Instead, the JU1395 background still
254 displayed a longer memory at high temperature in absolute time (Fig. 5B-C). We further
255 tested the RNAi memory of the N2 strain at 25°C versus 20°C. Similar to the JU1395
256 background, culturing N2 at the higher temperature resulted in an enhanced *gfp* RNAi
257 memory, in number of generations and in absolute time (Fig. S2B).

258 When facing harsh conditions during post-embryonic development, *C. elegans* can
259 arrest developmentally, and survive for several weeks without eating or reproducing (Hu,
260 2007; Baugh, 2013); when encountering new favorable conditions, normal growth can be
261 restored (Fig. 5A). For example, the L1 larval arrest arises after hatching in the absence of
262 food (Baugh, 2013). To reproduce this L1 developmental arrest, we let the first generation
263 after GFP RNAi exposure hatch in NGM plates without *E. coli* and remain for six days at 20°C,
264 as in Houri-Zeevi et al. (2021). L1 larvae were then fed again in standard conditions and RNAi
265 memory assayed. This early L1 arrest slightly reduces RNAi memory for the three tested
266 strains when counting in number of generations (Fig. 5D). Due to the time spent in L1 arrest,
267 when plotting in absolute time, RNAi memory was increased (Fig. 5E).

268 The stress-resistant dauer diapause, commonly found in *C. elegans* natural
269 populations (Schulenburg and Félix, 2017), corresponds to a specialized form of the early
270 third larval stage (Hu, 2007). Experimentally, dauer larvae can be obtained in conditions of
271 crowding, paucity of food and elevated temperature on young larvae (Karp, 2018). In order
272 to keep the conditions of RNAi initiation constant, we induced dauer larvae by letting the
273 first generation (G1) animals lay embryos without transfer to a new food source and
274 selected for dauers after a few days (see Methods). Passage through dauer for 5 days in the
275 second generation after RNAi initiation did not alter RNAi memory kinetics of the N2 and
276 JU1395 strains (Fig. 5F). Again, taking into account the diapause delay, passage through
277 dauer increased RNAi memory in absolute time (Fig. 5G). We further tested the long
278 memory background XZ1514 with dauer induction at 20°C, reproducing this procedure at
279 every generation after G2, and similarly did not see an effect of passage through dauer (Fig.
280 S2C). Thus, we conclude that the dauer stage, like the early L1 arrest, does not strongly
281 affect memory in number of generations and is able to maintain the memory of RNAi
282 through the days of diapause.

283 Bacteria that are found naturally associated with *C. elegans* encompass many
284 different genera (Dirksen et al., 2016; Samuel et al., 2016). We tested four such bacterial
285 wild isolates, *Leucobacter* CBX151, *Chryseobacterium* JUb044, *Acinetobacter* BIGb0102 and
286 *Comamonas* BIGb0172, selected for their ability to sustain *C. elegans* growth for multiple
287 generations while being potential pathogens (Hodgkin et al., 2013; González and Félix,
288 2024). We found that RNAi memory of the JU1395 and JU1171 wild backgrounds was
289 conserved relative to *E. coli* OP50, when cultured with these naturally-associated bacteria.
290 An exception is the JU1395 strain, which when tested on *Leucobacter* CBX151 displayed a
291 slight reduction in memory duration (Fig. S2A).

292 Discussion

293 We here provided evidence for microevolutionary variation in small RNA inheritance in *C.*
294 *elegans*. The duration of epigenetic inheritance can be treated as a quantitative trait in
295 theoretical (Helanterä and Uller, 2010; Day and Bonduriansky, 2011) and experimental
296 models of selection.

297 Natural genetic variation in RNAi inheritance

298 Like RNAi efficiency itself (Pollard and Rockman, 2013; Chou et al., 2024), the small RNA
299 inheritance trait is likely to have a polygenic basis. We provide evidence for polymorphisms
300 in several genes being involved, potentially acting at distinct points in the inheritance
301 mechanism. These may correspond to different parameters in mechanistic models of small
302 RNA memory, such as that developed by (Karin et al., 2023), which models feedback
303 amplification between small RNA and histone modifications, a resulting variation in mRNA
304 level, and a queuing system of small RNAs. Different molecular mechanisms for the
305 extinction of memory may be at stake as well (Shukla et al., 2021; Knudsen-Palmer et al.,
306 2024). Furthermore, after RNAi initiation, two phases have been experimentally
307 distinguished in transgenerational silencing, based on the mutation effect of different genes
308 in the N2 background (Woodhouse et al., 2018): establishment of RNAi inheritance at the
309 first generation and maintenance in further generations (Fig. S3).

310 The *drh-1* deletion allele seems to mildly diminish sensitivity to germline RNAi and
311 severely prevents RNAi inheritance (Fig. 3B, Fig. S4A). Memory may be simply affected by
312 the slightly lesser efficiency of the initial trigger, resulting in a less efficient initial
313 amplification. Alternatively, competition between small RNA pools along the generations
314 may be at stake, as seen with piRNAs or endosiRNAs, or as modeled by (Karin et al., 2023).
315 DRH-1 is a cytoplasmic protein (Batachari et al., 2024), expressed in both somatic and
316 germline cells (Wu et al., 2012). It recognizes preferentially blunt dsRNA (Consalvo et al.,
317 2024) and is involved in viral RNA recognition as well as a small RNA response to
318 mitochondrial stress (Mao et al., 2020). In an evolutionary context, *drh-1* polymorphism may
319 be driven by these different phenotypes alongside its effect on RNAi memory.

320 The *set-24* gene codes for a SET and SPK-domain protein, recently characterized by
321 Zeng, Furlan, Almeida et al. (2025). The SET-24 protein is localized to the germline nuclei.
322 Through its interaction with the epigenetic regulator HCF-1 and chromatin remodeling
323 complexes, SET-24 regulates H3K4me3 levels of hundreds of genes. Its dysregulation
324 perturbs the pools of inherited small RNAs, which leads to impaired inheritance and a
325 shorter RNAi memory (Zeng, Furlan, Almeida et al., 2025).

326 The *eri-6/7* locus quantitatively affects the maintenance of the memory, likely by
327 competition between pools of small RNAs, as modeled by Karin et al. (2023), whereby
328 amplification of endo-siRNAs requiring ERI-6/7 competes with other small RNA pools. The
329 partial inversion of the *eri-6/7* locus in the N2 background results in a hypomorphic allele (G.
330 Zhang et al., 2024), thus likely increasing RNAi memory. We note however that the only
331 strain with an ancestral single orientation *eri-7* locus in our set, XZ1514 (G. Zhang et al.,
332 2024), has a long memory so other variants elsewhere in the genome of this strain likely
333 affect the trait. It is likely that the variation in duration of small RNA memory is highly
334 polygenic in *C. elegans* wild strains.

335 336 Environmental effects on RNAi inheritance

337 Given the boom-and-bust lifecycle of *C. elegans* with a dispersal between food patches in
338 which the environment may differ (Félix and Duveau, 2012), we expected that starvation and
339 passage through the dispersal dauer stage may erase the small RNA memory. However, of
340 the different culture environments we tested during the memory phase, including dauer,
341 only temperature variation resulted in a large change, with an enhanced RNAi memory at
342 25°C compared to 20°C. This effect of temperature appeared after one generation of
343 initiation of the memory.

344 Houri-Zeevi et al. (2021) instead suggested that small RNA memory was 'reset' by
345 different stressing environments. They found a shortened memory, from the first
346 generation, after a transient heat shock (37°C). In contrast, they had previously shown that
347 inheritance of silencing relied on the activity of the heat-shock transcription factor HSF-1
348 (Houri-Zeevi et al., 2020), an effect that could be relevant in our experiments. *hsf-1*
349 overexpression leads to suppression of endogenous small RNA (sRNA) pathway components
350 and, likely due to competition among sRNA pools, a higher proportion of silenced progeny.
351 Using a 25°C temperature as a trigger rather than an environment during the memory phase,
352 others studies showed that this temperature altered siRNA pools for 3-4 generations (Schott
353 et al., 2014; Belicard et al., 2018) and de-repressed a silenced multi-copy fluorescent
354 reporter for over 10 generations (Klosin et al., 2017). Temperature is thus an ecologically
355 relevant factor initiating and modulating small RNA memory.

356 Concerning L1 stage starvation, Houri-Zeevi et al. (2021) reported a 'resetting' of
357 silencing memory, analyzing statistically each successive generation as if independent.
358 Following the same experimental procedure, and analyzing instead half-lives of silencing, we
359 observed a statistically significant yet mild difference on RNAi memory of *C. elegans*
360 between fed and starved conditions. Moreover, after halting development in the L1 or dauer
361 stages, silencing is maintained for a longer time in number of days. Knowing that *C. elegans*
362 in the wild remains in the dauer stage possibly for weeks in between nutrient-rich sources,
363 questions arise regarding the ecological relevance of memorizing conditions of a previous
364 environment.

365

366 **Conclusions and perspectives**

367 A transient epigenetic memory may be advantageous in environments that change on the
368 same timescale, with correlation between successive environments (Jablonka et al., 1995;
369 Lachmann and Jablonka, 1996; Rivoire and Leibler, 2014). In that case, the frequency of
370 environmental change and the life cycle duration of the organism will determine whether
371 multigenerational memory is advantageous. One can imagine the evolution of different
372 memory durations, with cases relying more on plasticity within a generation than on
373 inheritance. Using *C. elegans* experimental evolution, (Dey et al., 2016) showed that parental
374 effects could be selected in sequences of environments that vary at every generation. Our
375 findings of polymorphisms that affect small RNA inheritance will allow to test which
376 environmental sequences may favor one or the other allele. In addition, polymorphisms
377 affecting RNAi memory duration may be selected for a pleiotropic effect on another trait.
378 The prevalence of different forms of non-genetic inheritance across species highlights the
379 importance of evaluating experimentally how it itself evolves and might impact the course of
380 evolution.

381 **Materials and methods**

382

383 ***C. elegans* culture and strains**

384 *C. elegans* was cultured on 55 mm NGM agar plates (Stiernagle, 2006) seeded with 100 µl
385 of a saturated culture of *E. coli* OP50 grown overnight in Luria Broth (LB) at 37°C, except if
386 otherwise indicated. *C. elegans* wild isolates were obtained from the Caenorhabditis
387 Genetics Center (CGC), Michael Ailion, Erik Andersen, Leonid Kruglyak or our own collection.
388 The *set-24(bab562)* and *drh-1(bab552)* mutants were engineered using CRISPR/Cas9 editing
389 by the CNRS SEGICel facility (Lyon, France), mimicking the natural alleles characterized in
390 Frézal et al. (2018) and Ashe, Bécicard, Le Pen, Sarkies et al. (2013), respectively. The
391 *eri-6(mg379)* mutant (Fischer et al., 2008) was obtained from the CGC. Bleaching of cultures
392 was performed as in Hibshman, Webster et al. (2021).

393

394 ***E. coli* strains and plasmids**

395 The *gfp* targeting sequence directed against the *pie-1p::GFP* transgene was obtained from
396 Eric Miska's laboratory and inserted into the L4440 vector. The *gfp* targeting sequence
397 directed against the *mex-5p::ce-GFP* transgene was inserted into plasmid L4440 (Timmons et
398 al., 2001), yielding plasmid pMNK25. The NotI-KpnI digested insert was subcloned into the
399 T444T plasmid (Sturm, Saskoi et al., 2018), yielding plasmid pFF1, the latter harboring
400 transcriptional terminators (Table S4). The RNAi clone that was used is indicated for each
401 experiment. In our first experiments, *E. coli* bacterial strains HT115 was used transformed
402 with plasmid pMNK25 and in later experiments, *E. coli* iOP50 was used with pFF1. The latter
403 combination seems to result in a stronger RNAi efficiency, but the overall variation among
404 strains is comparable for all clones.

405

406 **Bacterial strains**

407 The non-*E. coli* bacteria were originally isolated from different *Caenorhabditis* collected in
408 the wild. CBX151 *Leucobacter* was found infecting a *Caenorhabditis* collected in Cape Verde
409 (Hodgkin et al., 2013). JUb044 *Chryseobacterium* was isolated from Santeuil, France;
410 BIGb102 *Acinetobacter* and BIGb172 *Comamonas* were collected in decomposing apples in
411 Orsay, France (Samuel et al., 2016). These bacteria were grown in LB liquid culture for 16
412 or 32 h with 220 rpm agitation at 22°C for CBX151 or 28°C for the other bacteria.

413

414 **Introgression of the *pie-1p::GFP::H2B::pie-1* transgene**

415 We initially used the *mjls31[pie-1p::GFP::H2B]* transgene (Ashe, Sapetschnig et al., 2012),
416 introduced by MosSCI (Frøkjær-Jensen et al., 2008) in the reference strain N2 on
417 chromosome II at 8.4 Mb, yielding strain SX461 (Ashe, Sapetschnig et al., 2012). As this
418 transgene is easily silenced, we first desilenced its expression using *mut-7* RNA interference.
419 We then introgressed the transgene in several wild isolates by at least six rounds of
420 backcrossing to the target wild genetic background, using SX461 males in the first cross. The
421 primers used to verify the genotype of the different chromosomes are in Table S5 for
422 JU1171, MY10 and JU775, with specific attention to the presence of *set-24(mfp23)II* in the
423 MY10 genetic background; genotyping was not performed for JU1395 because of its close
424 relatedness to N2. As this transgene was introduced in different wild isolates through
425 backcrosses (Ashe, Sapetschnig et al., 2012), a N2 genomic segment linked to it is also
426 present and of a different length for each backcross. As these N2 genomic regions could in
427 principle affect RNAi memory compared to the target wild genomic background, we also

428 used CRISPR/Cas-9 genome editing to introduce the transgene at a given locus,
429 circumventing this problem.

430

431 **Introduction of the *mex-5p::ce-GFP::tbb-2 3'UTR* transgene by genome editing**

432 A CRISPR-Cas9 protospacer was selected (TCCGTGTCTTACTACTGTA) in a conserved region on
433 chromosome I that is permissive for germline expression (El Mouridi et al., 2022). The
434 protospacer was added to an sgRNA(F+E) scaffold (Chen et al., 2013) and ordered as a gene
435 fragment (Twist Bioscience, CA, USA). The gene fragment was subsequently cloned into an
436 empty ampicillin resistant vector using Gibson assembly (Gibson et al., 2009) to give
437 pMDJ344. An expression vector containing a *mex-5* promoter (pCFJ645) (Zeiser et al., 2011),
438 a nuclear *C. elegans*-optimized GFP (pCFJ2389) (Aljohani et al., 2020), a *tbb-2* 3'UTR
439 (pCM1.36) (Merritt et al., 2008), and a hygromycin resistance cassette (pCFJ767) (Radman et
440 al., 2013) were cloned using a multi-site Gateway reaction (Invitrogen cat. no. 12538200) to
441 give pMDJ343. Roughly 250 bp homology arms from either end of the selected CRISPR-Cas9
442 cut site were added to pMDJ343 using Gibson assembly (Gibson et al., 2009) to make the
443 final repair template pMDJ346. The resulting lines are listed in Table S1.

444 A similar procedure was performed exclusively on an N2 genetic background, this
445 time using a (CCGTGGAATCAAGTTAATC) CRISPR-Cas9 protospacer in a conserved region of
446 chromosome V. By using the same methodology as stated above, the resulting gene
447 fragment cloned into an empty ampicillin resistant vector gave pMDJ345. The adding of 250
448 bp homology arms from either end of this chromosome V cut site to the *mex-5p::ce-*
449 *GFP::tbb-2* transgene and its hygromycin resistant cassette gave pMDJ347. This insertion
450 was used to cross the *eri-6* mutation located on chromosome I.

451 Injection mix contained a codon-optimized Cas9 expression vector (pCFJ2474)
452 (Aljohani et al., 2020) at 25 ng/μl, the sgRNA vector (pMDJ344) at 5 ng/μl, the repair
453 template (pMDJ346) at 10 ng/μl, a linearized histamine marker (pSEM238) (El Mouridi et al.,
454 2021) at 10 ng/μl, a pan-muscular mCherry marker (pSEM235) (El Mouridi et al., 2020) at 10
455 ng/μl, and a DNA ladder (1 kb plus, Invitrogen) at 40 ng/μl to make up a final mix
456 concentration of 100 ng/μl. 10-20 young adults were injected for each wild isolate as
457 previously described (Mello et al., 1991) and placed at 20°C. 500 μl of hygromycin (4 mg/ml)
458 was added three days post injection to select for extrachromosomal array animals (Radman
459 et al., 2013). Once plates starved (7 days post injection), 500 μl of histamine (500 mM) were
460 added to paralyze extrachromosomal array animals (El Mouridi et al., 2021). Single copy
461 insertion lines are characterized by hygromycin resistance, insensitivity to histamine, lack of
462 somatic mCherry fluorescence, and germline *ce-gfp* expression.

463

464 **Comparison between the transgenes**

465 The *pie-1p::GFP* transgene possesses three introns and four exons. Sequence of *gfp* in the
466 *mex-5::ce-GFP* transgene is around 1.75 kb and possesses six introns and five exons.

467 The *mex-5p::ce-GFP* transgene was custom-built for this work. It includes an
468 engineered *gfp* sequence that was designed to lack piRNA homology sites and favor
469 transgene expression (Aljohani et al., 2020). We cannot rule out that the piRNA loci differ
470 among the *C. elegans* wild isolates and that for example some of the long memory strains
471 possess piRNAs targeting this transgene. However, we note that the same ranking of wild
472 strains regarding RNAi memory was observed with the *pie-1p::GFP* transgene, which has a
473 quite different sequence, which only matches that of the *mex-5p::ce-GFP* transgene on

474 571/792 nucleotides along the mRNA. For RNAi, we used *E. coli* produced dsRNAs (Table S4)
475 with a perfect match against the length of the corresponding mRNA.

476

477 **Culture plates for RNAi interference**

478 Empty 55 mm Petri dishes were poured with autoclaved NGM medium supplemented with a
479 2 μ m filtered IPTG solution to obtain a final concentration of 1 mM. Plates were left to dry
480 overnight and covered at room temperature. In parallel, liquid cultures of dsRNA vector
481 containing-bacteria were incubated for ~16 hrs at 37°C with agitation at 220 rpm. The next
482 day, the bacterial liquid cultures were used to seed now solidified NGM-IPTG plates with 100
483 μ L and left to dry overnight covered at room temperature. This process was repeated for the
484 two generations of exposure to RNAi (G-1 and G0).

485

486 **GFP silencing memory assay**

487 Stock populations of GFP+ nematodes were maintained for at least three generations at
488 15°C before starting an experiment. Three replicates were conducted in parallel for each.
489 RNAi was initiated 20°C by randomly picking three L4 stage individuals from the stock
490 populations onto RNAi plates. Three L4 stage larvae derived from these founders
491 (designated generation G-1) were randomly chosen for transfer onto fresh RNAi plates. In
492 block A, 60 L4 larvae of the next (G0) generation were transferred from the RNAi memory
493 environment to standard conditions, without RNAi trigger. For all other blocks, the G0 adults
494 were treated with a “bleach” solution (Hibshman et al., 2021) to break down their cuticle
495 and isolate their embryos, thus killing dsRNA expressing bacteria. Embryos were then
496 deposited onto standard 20°C NGM plates seeded with saturated OP50 *E. coli*, unless
497 indicated otherwise. These embryos were designated as generation G1. At each generation,
498 60 random L4 stage individuals were passed to produce the next generation and the
499 remaining population chunked onto a fresh new NGM-OP50 plate to avoid starvation. The
500 next day, the chunked population was scored and the transferred individuals were removed
501 and their progeny allowed to grow.

502 Changes in the environment were performed during the memory phase, thus after
503 the initiation step of parental RNAi exposure at 20°C in G-1 and G0.

504 *Temperature:* After the initiation step, subsequent generations were cultured at 25°C
505 or 20°C on standard NGM medium seeded with 100 μ L of saturated *E. coli* OP50 culture.

506 *Bacteria:* After the initiation step, subsequent generations were cultured at 20°C in
507 standard NGM medium seeded with 100 μ L of saturated cultures of the tested bacteria.

508 *Starvation:* After the initiation step, the bleach-treated embryos were deposited onto
509 an empty NGM plate and left to starve for 6 days at 20°C. At this time point, L1 larvae were
510 collected in M9 solution, centrifuged 1 min at 3000 rpm and transferred to standard culture
511 plates to resume their development and continue the GFP silencing memory experiment as
512 described above.

513 *Dauer:* In order to keep the conditions of RNAi initiation constant, we induced dauer
514 larvae by letting the first-generation animals lay embryos without transfer to a new food
515 source. Specifically, after initially transferring 60 L4 stage G1 individuals onto new plates for
516 the fed control, the remaining population was separated in two, half being fed for scoring of
517 the G1 generation and the other half left on the plate. The latter was then placed at either
518 20°C or 25°C for 7 and 5 days, respectively, in order to obtain a mix of L1/L2 arrest and dauer
519 larvae of the next generation. 1% sodium dodecyl sulfate (SDS) was then used to filter out
520 dauer individuals from the rest by ~20 min incubation with mellow agitation (Karp, 2018).

521 Surviving dauer larvae were then deposited back onto standard culture plates to resume
522 development and continue the assay.

523

524 **Microscopy and GFP expression quantification**

525 Animals harboring the *pie-1p::GFP* transgene were scored using a Zeiss AxioImager M1
526 microscope with a x63 objective and a Semrock GFP-1828A-000 filter. Animals harboring the
527 *mex-5p::ce-GFP* transgene were scored using a Nikon AZ100 fluorescence microscope with a
528 5x objective and level 3 zoom and a Semrock GFP-3035D filter. Hermaphrodite adults were
529 collected using M9 solution and pelleted waiting ~2 minutes. A 15 μ L drop of pelleted
530 nematodes was deposited on a microscope slide containing a thin layer of 4% agar noble gel
531 supplemented with 100 μ M of NaN_3 . Around 100 individuals were scored for each replicate
532 using no transillumination light. During the silencing recovery period, with the *pie-1p::GFP*
533 transgene, nematodes were considered "OFF" when both arms were silenced or "ON" when
534 at least one mature oocyte presented nuclear fluorescence. With the *mex-5p::ce-GFP*
535 transgene, intensity and site of GFP expression varied among individuals leading us to sort
536 nematodes according to their GFP pattern and brightness levels into "OFF", "DIM" or "ON"
537 categories. OFF individuals were those showing no nuclear fluorescence in their gonad, DIM
538 individuals were those with varied patterns of expression but no nuclear fluorescence in
539 their proximal gonad and ON individuals expressing GFP+ meiotic oocyte nuclei. Results with
540 these three categories are shown in Table S2 and Figure Sn. The OFF and DIM categories
541 were grouped for plotting and analysis as we considered that DIM individuals were still
542 inheriting RNAi.

543

544 **Half-life of GFP RNAi memory and statistical analysis**

545 We calculated the GFP RNAi memory half-life values arithmetically based on the raw scoring
546 counts presented in Table S2. For every replicate of every strain in every block, we selected
547 the two scoring time points for which the percentage of GFP-positive individuals were the
548 closest below and above 50, respectively, and calculated the corresponding line equation.
549 Based on this equation, we obtained the theoretical median value of GFP RNAi memory
550 allowing us to generate the boxplots shown in Fig. 1E, Fig. 2B, Fig. 3C, Fig. 4D and Fig. S1 and
551 to conduct statistical analysis. For values oscillating around the median line, a smoothing
552 was realized picking scoring time points further apart. Raw values and indications can be
553 found in Table S3.

554 Generalized linear mixed model (GLMM) were fit using the *glmmTMB* (v.1.1.10)
555 package in the R version 4.2.2 (2022-10-31) to compare differences in half-life of GFP RNAi
556 memory across strains or environments.

557 The model we used to test for the effect of genetic variation was:

```
558 model_1 <- glmmTMB(Value ~ Strain + (1|Block) + (1|Block:Replicate),  
559                   family = Gamma(link = "log"), data = data)
```

560 The model we used to test for the effect of an environmental variable was:

```
561 model_2 <- glmmTMB(Value ~ Strain*Environment + (1|Block) + (1|Block:Replicate),  
562                   data = data)
```

563 We used the *emmeans* package (v.1.10.6) and Tukey's post-hoc test for pairwise
564 comparison, either among strains:

```
565 emmeans(model, pairwise ~ Strain, adjust = "tukey")
```

566 or between environments for a given strain:

```
567 emmeans(model, pairwise ~ Environment|Strain, adjust = "tukey")
```

568

569 For blocks realized only once, the random variable (1|Block) was removed from the model.
570 All models were validated by fitting the DHARMA package (v.0.4.7) simulations.

571

572 **Haplotype tree building and genetic relatedness**

573 We downloaded the 611 hard-filtered Variant Call Format (VCF) file from CaENDR (20220216
574 release) (Cook et al., 2017) from which we extracted the data for our eight strains of
575 interest. We converted this VCF file to a PHILIP file using the *vcf2phylip.py* script (Ortiz,
576 2019). The haplotype network was generated using this PHILIP file and the SplitsTree
577 software (v6.4.13) (Huson and Bryant, 2006).

578 Presence of the *drh-1* 159 bp deletion among the 611 hard-filtered isotypes was
579 detected using BCFtools (v1.9) and manually checked via CaENDR's genome browser tool.
580 Sampling location for each *C. elegans* isotype was downloaded from CaENDR (20231213
581 data release).

582

583 **Acknowledgements**

584 We are grateful to Hervé Gendrot for plate pouring and to Aurélien Richaud for laboratory
585 management. We thank Katie Pelletier for help with statistical analysis. We thank Eric Miska,
586 Germano Cecere and members of the Félix lab for discussions. Some strains were provided
587 by the CGC, which is funded by NIH Office of Research Infrastructure Programs (P40
588 OD010440). We thank the SEGiCel genome editing platform (CNRS, Lyon), especially Arnaud
589 Echard and Margaux Gibert. We thank Wormbase and CaENDR. This work was supported by
590 grants from the Agence Nationale pour le Recherche ANR-19-CE12-0025-01 and ANR-24-
591 CE12-0362-01. For the purpose of Open Access, the author has applied a CC BY public
592 copyright licence to any Author Accepted Manuscript version arising from this submission.

593

594 **Author contributions**

595 M.-A.F. and L.F. designed the project; L.F. performed the introgressions and developed
596 protocols; C. F.-J. provided reagents; M. A. made genome edits for transgene insertion; F.F.,
597 M.S. and L.F. performed RNAi memory assays; F.F. performed the statistical analyses and
598 made the figures; F.F., M.-A.F. and M.S. wrote the manuscript with contributions and edits
599 of all authors; M.-A. F. supervised the project, with contributions from L.F. and C. F.-J.
600

601 **Figure legends**

602

603 **Figure 1: Variation in the duration of RNAi memory among *C. elegans* natural isolates.**

604 **(A)** Haplotype network of the *C. elegans* natural isolates used in this work. The network is
605 based on genome-wide single-nucleotide polymorphisms from CaENDR (Crombie et al.,
606 2019) and built using SplitsTree.

607 **(B)** Introduction of germline-expressed transgenes into *C. elegans* natural isolates, either
608 through introgression by successive backcrosses or introduction at the same genomic site by
609 CRISPR/Cas9-mediated editing. The two transgenes differ in *cis*-regulatory sequences, coding
610 sequences and 3'UTR. The *pie-1p* transgene drives expression of GFP fused to histone H2B.
611 The *mex-5p* transgene drives expression of a *ce-GFP* sequence with two NLS sequences and
612 is devoid of predicted piRNA sites. The fluorescence micrographs show their different
613 patterns of GFP expression. Bar: 100 μ m for both pictures.

614 **(C)** Schematic of the GFP silencing memory assay. RNAi is triggered by feeding a stock of
615 animals expressing GFP (as indicated by the green color) with *E. coli* bacteria expressing
616 double-stranded RNA against the corresponding GFP sequence for two generations (called
617 G-1 and G0). The two transgenes strongly differ in coding sequences, and thus distinct RNAi
618 clones were used to silence each transgene. Experimental variations during RNAi initiation or
619 the memory assay are indicated.

620 **(D)** Four independent experiments assaying RNAi memory variation in different isolates with
621 the *mex-5p::ce-GFP::tbb-2* transgene inserted on chromosome I. We call each of these four
622 independent experiments a block, lettered here C, D, E and F. Three replicates were run for
623 each line for each block (see Table S2 for raw results). In these experiments, RNAi was
624 initiated with *E. coli* HT115 bacteria transformed with pMNK25. For the sake of simplicity, we
625 indicate the name of the wild isolate background rather than that of the genome-edited
626 strain (see Table S1 for the corresponding strain name). The rank order of the strains is
627 highly reproducible. On the graph, the lines follow the means of the three replicates and
628 error bars represent their standard deviation (SD).

629 **(E)** Boxplot showing the estimated half-lives of *gfp* silencing memories extracted from the
630 data in (D) (see Table S3 for raw values). Generalized linear mixed-model (glmm) statistics
631 based on these values (excluding strains tested once) demonstrated a strong effect of the
632 strain on the dynamics of *gfp* desilencing over generations: $p < 2 \times 10^{-16}$.

633

634 **Figure 2: A natural DNA sequence polymorphism in the *set-24* gene affects RNAi memory.**

635 **(A)** Effect on RNAi memory of the *set-24(bab562)* allele using the *mex-5::ce-GFP* transgene in
636 the N2 genetic background. The four panels correspond to the same four blocks as in Fig. 2A.
637 Lines of each graph follow the mean of three replicates and the bars represent the standard
638 deviation of the replicates.

639 **(B)** Boxplot showing the estimated half-lives of GFP RNAi memory. Glmm analysis based on
640 these values followed by a Tukey pairwise comparison indicates a statistical difference for
641 the median RNAi silencing memory between N2 and the strain carrying the *set-24(bab562)*
642 allele in N2 background: $p < 1 \times 10^{-4}$, as well as between the latter and the MY10 strain: $p <$
643 1×10^{-4} .

644 **(C)** Schematic depicting the *set-24* gene and the location of the natural deletion in the MY10
645 genetic background.

646

647 **Figure 3: A common natural DNA sequence polymorphism in the *drh-1* gene affects RNAi**
648 **sensitivity and memory.**

649 **(A)** Diagram depicting the proportion of isotypes possessing the 159 bp deletion in *drh-1* by
650 world region. Numbers shown correspond to the number of isotypes sequenced by
651 continent from CaenDR. As no isolate sampled in Hawaii presents this polymorphism, Hawaii
652 was excluded from the representation. Created with BioRender.com.

653 **(B)** Effect on RNAi memory of the *drh-1(bab552)* allele using the *mex-5::ce-GFP* transgene in
654 the N2 genetic background. Panels correspond to blocks N and O. In these two blocks, *E. coli*
655 iOP50 bacteria transformed with pFF1 (see Methods) were used to initiate RNAi against *gfp*.
656 Lines of each graph follow the mean of three replicates and the bars represent the standard
657 deviation of the replicates.

658 **(C)** Boxplot showing the estimated half-lives of GFP RNAi memory of the strains tested in
659 blocks N and O. Glmm analysis based on these values followed by a Tukey pairwise
660 comparison indicates a statistical difference for the median RNAi silencing memory between
661 N2 and *drh-1(bab552)* in N2: $p = 1.1 \times 10^{-3}$; between MY10 and *drh-1(bab552)* in N2: $p < 1 \times 10^{-4}$.
662

663

664 **Figure 4: Competition between endogenous and exogenous small RNA pathways alters**
665 **RNAi memory duration.**

666 **(A)** Diagrams depicting two commonly found gene structures of the *eri-6/7* locus in *C.*
667 *elegans* wild strains (here additional introns within each large block are omitted). The
668 ancestral state of this locus harbors a unique gene in the right to left orientation (colored in
669 blue). The more recent N2-like structure of *eri-6/7* is thought to have arisen from a
670 transposable element invasion, a resulting inversion of the first exons (pink orientation, left
671 to right) forming the so-called *eri-6* part of the gene. This rearrangement of *eri-6*
672 is predominant in isolates outside of Hawaii and is hypomorphic (Fischer, Butler et al., 2008; G.
673 Zhang et al., 2024).

674 **(B)** Diagram showing the detailed gene structure of *eri-6* as found in the N2 genetic
675 background. The laboratory *mg379* allele is a splice-donor mutation.

676 **(C)** RNAi memory assay (blocks K and L) of the *eri-6(mg379)* mutant, using the *mex-5p::ce-*
677 *GFP* transgene. This *eri-6* reduction-of-function mutation decreases endogenous small RNA
678 production, thus enabling a better amplification of 2° siRNAs corresponding to exogenous
679 dsRNAs and leads to a longer RNAi memory. *E. coli* iOP50 was used to initiate *gfp* RNAi.

680 **(D)** Boxplot showing estimated half-lives of GFP RNAi memory for N2 and *eri-6(mg379)* in
681 blocks K and L. Glmm on these half-life values followed by a Tukey pairwise test indicates a
682 statistical difference of median RNAi silencing memory between strains: $p < 1 \times 10^{-4}$.

683 **(E)** World map presenting the percentage of isotypes possessing either one of the *eri-6/7*
684 gene structures shown in (A) relative to the total number of isotypes by world region in
685 CaenDR. Other structures of this locus comprise, for example, a single *eri-6/7* gene without
686 *sosi-1* and *eri-6[e][f]* genes, *eri-6[exons]* surrounded by remnants of the transposable
687 element and an N2-like structure with duplicated *eri-6[exons]* (G. Zhang et al., 2024). Created
688 with BioRender.com.

689

690 **Figure 5: Impact of the environment on the duration of RNAi memory.**

691 **(A)** Schematic illustration of the “boom-and-bust” life cycle of *C. elegans* natural populations
692 (created with BioRender.com).

693 **(B-G)** Tests of temperature [B-C], L1 arrest [D-E] and dauer diapause [F-G] on RNAi memory
694 duration using the *mex-5p::GFP* transgene, initiating RNAi against *gfp* with *E. coli* iOP50
695 bacteria transformed with pFF1. The results are plotted along the number of generations in
696 [B, D, F] and number of days in [C, E, G]. For each block and condition, 3 replicates were run
697 per strain. Graph lines represent means and bars the standard deviation.

698 **(B-C)** Effect of temperature on RNAi memory in the JU1171 and JU1395 backgrounds (block
699 G). Culturing JU1395 at 25°C increases duration of its RNAi memory in number of
700 generations (glmm on half-lives of GFP RNAi memory in blocks C and G, $p < 1 \times 10^{-4}$) and in
701 days ($p = 5.3 \times 10^{-3}$). No significant difference was observed for JU1171. See Fig. S2B for an
702 additional experiment using the N2 and JU1395 backgrounds.

703 **(D-E)** Effect of L1 arrest for 6 days at 20°C at the first generation after parental RNAi
704 exposure for strains in the N2, JU1395 and XZ1514 backgrounds (block L). Analyzing the half-
705 lives of the GFP RNAi memory of N2 and JU1395 in blocks K and L in a glmm framework, a
706 significant reduction between control and starvation conditions were found in generations, p
707 = 2.8×10^{-3} and 5×10^{-4} , for N2 and JU1395, respectively, as well as a significant extension of
708 RNAi memory in absolute time, $p < 1 \times 10^{-4}$ for each strain.

709 **(F-G)** Effect of a ~3-day long dauer diapause at the second generation after GFP RNAi
710 exposure (block M). No effect was found on GFP de-silencing dynamics when expressing the
711 results in number of generations (glmm on half-lives, followed by Tukey's test, $p > 0.45$
712 between fed and dauer condition for both N2 and JU1395). However, the RNAi memory was
713 extended in number of days after passage through dauer in G2 in the JU1395 background (p
714 = 5.6×10^{-3} between fed and dauer conditions). This experiment was performed at 25°C.

715 **Supplementary figure legends**

716

717 **Figure S1: The rank order of memory duration of wild background strains is overall**
718 **conserved when using the two distinct GFP transgenes.**

719 **(A)** GFP silencing memory assay comparing in parallel the RNAi memory duration of the
720 reference strain N2 with either the *pie-1p::GFP::H2B* or the *mex-5p::ce-GFP* transgenes. *E.*
721 *coli* HT115 with the relevant *gfp* sequence clone for each transgene was fed to initiate RNAi
722 against *gfp*. Three biological replicates were run for each strain, scoring the proportion of
723 GFP-positive (GFP+) animals at each generation. On the graph, the lines follow the means of
724 three replicates and error bars represent their standard deviation (SD).

725 **(B)** Boxplot showing the GFP RNAi memory half-lives of a N2 genetic background with the
726 *mex-5p::ce-GFP* or *pie-1p::GFP* transgenes. Half-lives were estimated from the scoring data
727 shown in (A).

728 **(C)** Diagram depicting the two *gfp* transgenes used in this study. The *pie-1* promoter is 2 kb
729 long and not represented to scale. The two transgenes strongly differ in terms of cis-
730 regulatory and coding sequences.

731 **(D)** Two independent experiments assaying the RNAi memory duration of the same wild
732 isolates containing either the *pie-1p::GFP::H2B* (Block A) or *mex-5p::ce-GFP* (Block C, also
733 plotted in Fig. 2) transgenes. For both blocks, *E. coli* HT115 was fed to initiate RNAi against
734 *gfp*. As the *pie-1p::GFP* experiment only tested the MY10, JU1171, JU775, N2 and JU1395
735 backgrounds, only the relevant strains are plotted for *mex-5p::ce-GFP*. The variation in
736 memory of the wild strains is overall conserved when using the two distinct GFP transgenes.

737 **(E)** Boxplots showing the GFP RNAi memory half-lives of the MY10, JU1171, JU775, N2 and
738 JU1395 backgrounds with either GFP transgene. As expected, the memory is longer with the
739 *pie-1p::GFP::H2B* where piRNA recognition sites have not been avoided.

740

741 **Figure S2: Effect of additional culture environments on the duration of RNAi memory.**

742 **(A)** Three different experiments (blocks H, I and K) testing for the effect of *Chryseobacterium*
743 JU044, *Acinetobacter* BIGb102, *Comamonas* BIGb172 and *Leucobacter* CBX151 on RNAi
744 memory. Here the moderate-memory strain JU1395 or low-memory strain JU1171
745 containing the *mex-5::ce-GFP::tbb-2* transgene were fed with *E. coli* iOP50 to initiate *gfp*
746 RNAi. No striking differences were observed in RNAi memory profile between *E. coli* OP50 or
747 naturally associated bacteria except for a reducing effect of CBX151 on the nematode strain
748 JU1395. Statistics comparing estimated GFP memory half-lives of a given strain in different
749 bacterial condition to the OP50 control: glmm followed by Tukey's comparison against OP50:
750 $p > 0.06$ for each bacterial strain on JU1171 and $p > 0.3$ for each bacterial strain on JU1395
751 except with CBX151, $p = 0.02$. As no major delay was seen in development or egg laying
752 under these conditions, generation time and absolute time are equivalent.

753 **(B)** The panels correspond to the same block L (distinct from the experiment shown in Figure
754 4B-C) testing for effect of temperature on RNAi memory in the strains JU1395 and N2
755 containing the *mex-5p::ce-GFP::tbb-2* transgene and fed with *E. coli* iOP50 to initiate *gfp*
756 RNAi. Data were plotted either in number of generations or days after RNAi initiation.

757 **(C)** Independent block J testing for the effect on RNAi memory kinetics of dauer diapause
758 induced at different generations. The long-memory strain XZ1514 containing the *mex-5p::ce-*
759 *GFP::tbb-2* transgene was fed with *E. coli* iOP50 to initiate *gfp* RNAi. This experiment was
760 performed at 20°C. Dauer individuals of a given generation were induced by letting parents
761 of the previous generation lay eggs and not re-supplying plates with *E. coli* OP50. Individuals

762 were left for ~3 days in the dauer stage. This was performed at every generation by
763 separating in half the control individuals as population to be scored (fed) or population to lay
764 (not fed) (see Methods). Dauer larvae were selected by incubation of the whole population
765 in 1% sodium dodecyl sulfate (SDS) for ~20 minutes at room temperature with moderate
766 agitation before being deposited back onto standard NGM-OP50 plates to resume
767 development. The dauer diapause does not greatly affect further GFP silencing memory
768 dynamics when expressed in number of generations.

769

770 **Figure S3: Sensitivity to RNAi exposure is lower in the *C. elegans* MY10 strain but the *set-*
771 **24** mutation in the N2 background only affects memory.**

772 Block F including *gfp* silencing dynamics during RNAi initiation. Starting from a 15°C stock
773 population where every individual expresses GFP fluorescence, the two-generation (G-1 and
774 G0) of GFP RNAi exposure leads to full GFP silencing except in the MY10 strain. Are shown in
775 the graph the different phases of the *gfp* silencing inheritance process with initiation of *gfp*
776 RNAi, establishment of RNAi inheritance, and maintenance of RNAi inheritance.

777

778 **Figure S4: Efficiency of *gfp* RNAi initiation in wild strains and the *drh-1* mutant.**

779 **(A)** Block N showing the dynamics of *gfp* silencing (generations G-1 and G0) in the MY10,
780 JU1171, N2, *drh-1(bab552)* in N2, and JU1395 backgrounds harboring the *mex-5p::ce-GFP*
781 transgene and fed with *E. coli* iOP50 for RNAi initiation. The *drh-1* natural deletion allele
782 reduces both responsiveness to *gfp* RNAi as well as RNAi memory.

783 **(B)** Microscopy images illustrating GFP silencing and desilencing dynamics of wild isolates
784 through time. GFP microscopy images from block N taken in parallel with the scoring. Before
785 *gfp* RNAi, stock populations of all four natural strains show identical patterns of GFP
786 expression. Use of iOP50 with a T444T cassette seems to enhance efficiency of RNAi as even
787 MY10 is almost fully silenced for *gfp* at G0. At the first generation after RNAi exposure,
788 almost the whole populations of MY10 and JU1171 recover fluorescence while populations
789 of N2 and JU1395 retain some silencing. Dots in the pharynx of silenced individuals are due
790 to autofluorescence.

791 **Supplementary tables**

792

793 **Table S1: List of nematode strains used in this paper.**

794 List of wild *C. elegans* isolates and their derived transgene-modified counterparts with their
795 origin and method of construction.

796

797 **Table S2: Raw scoring data of GFP silencing memory assay.**

798 Each block corresponds to an independent experiment. DIM and OFF individuals were
799 pooled for simplicity in the graphs. Plasmid code names and bacteria used for GFP RNAi
800 exposure are detailed in Table S4.

801

802 **Table S3: Values of GFP RNAi memory half-lives.**

803 Half-lives of GFP memory were calculated based on the raw scoring counts presented in
804 Table S2 (see methods for procedure). A slash mark in the column for half-lives counted as
805 days corresponds to cases with no difference between the time expressed in generation
806 number or in days. For rare line plots values crossing the 50° value twice, a smoothing of the
807 linear RNAi memory tendency was performed, and indicated by an arrow showing the
808 selected data points.

809

810 **Table S4: Bacterial strains and transgenes used in this paper.**

811 The first sheet shows the list of *C. elegans* naturally associated-bacteria used as testing
812 environments as well as artificial *E. coli* strains used for RNAi induction. The second sheet
813 shows the sequences of *gfp* transgenes and their corresponding targeting dsRNA.

814

815 **Table S5: Genotyping of the *pie-1p::GFP* transgene introgressions.**

816 As the JU1395 and N2 genetic backgrounds are closely related to each other, we only used
817 primers that could distinguish deletions in the MY10, JU775 and JU1171 isolates compared
818 to N2.

819 **Bibliography**

820 *: equal contribution. # correspondence (omitted if last author only)

821

822 Adrian-Kalchhauser, I., Sultan, S. E., Shama, L. N. S., Spence-Jones, H., Tiso, S., Keller
823 Valsecchi, C. I., et al. (2020). Understanding “non-genetic” inheritance: insights from
824 molecular-evolutionary crosstalk. *Trends Ecol. Evol.* 35, 1078–1089. doi:
825 10.1016/j.tree.2020.08.011

826 Ahmed, S.#, and Hodgkin, J. (2000). MRT-2 checkpoint protein is required for germline
827 immortality and telomere replication in *C. elegans*. *Nature* 403, 159–164. doi:
828 10.1038/35003120

829 Aljohani, M. D.*, El Mouridi, S.*, Priyadarshini, M.*, Vargas-Velazquez, A. M.*, and Frøkjær-
830 Jensen, C. (2020). Engineering rules that minimize germline silencing of transgenes in
831 simple extrachromosomal arrays in *C. elegans*. *Nat. Commun.* 11, 6300. doi:
832 10.1038/s41467-020-19898-0

833 Ashe, A.*, Béliard, T.*, Le Pen, J.*, Sarkies, P.*, Frézal, L., Lehrbach, N. J., et al. (2013). A
834 deletion polymorphism in the *Caenorhabditis elegans* RIG-I homolog disables viral
835 RNA dicing and antiviral immunity. *eLife* 2, e00994. doi: 10.7554/eLife.00994

836 Ashe, A., Colot, V., and Oldroyd, B. P. (2021). How does epigenetics influence the course of
837 evolution? *Philos. Trans. R. Soc. Lond. B. Biol. Sci.* 376, 20200111. doi:
838 10.1098/rstb.2020.0111

839 Ashe, A.*, Sapetschnig, A.*, Weick, E.-M.*, Mitchell, J.*, Bagijn, M. P., Cording, A. C., et al.
840 (2012). piRNAs can trigger a multigenerational epigenetic memory in the germline of
841 *C. elegans*. *Cell* 150, 88–99. doi: 10.1016/j.cell.2012.06.018

842 Batachari, L. E., Dai, A. Y., and Troemel, E. R. (2024). *Caenorhabditis elegans* RIG-I-like
843 receptor DRH-1 signals via CARDs to activate antiviral immunity in intestinal cells.
844 *Proc. Natl. Acad. Sci.* 121, e2402126121. doi: 10.1073/pnas.2402126121

845 Baugh, L. R. (2013). To grow or not to grow: nutritional control of development during
846 *Caenorhabditis elegans* L1 arrest. *Genetics* 194, 539–555. doi:
847 10.1534/genetics.113.150847

848 Baugh, L. R.#, and Day, T. (2020). Nongenetic inheritance and multigenerational plasticity in
849 the nematode *C. elegans*. *eLife* 9, e58498. doi: 10.7554/eLife.58498

850 Béliard, T., Jareosettasin, P., and Sarkies, P. (2018). The piRNA pathway responds to
851 environmental signals to establish intergenerational adaptation to stress. *BMC Biol.*
852 16, 103. doi: 10.1186/s12915-018-0571-y

853 Billi, A. C., Fischer, S. E. J., and Kim, J. K. (2014). Endogenous RNAi pathways in *C. elegans*.
854 *WormBook Online Rev. C. elegans Biol.*, 1–49. doi: 10.1895/wormbook.1.170.1

855 Bondurianski, R., Day, T. (2018). Extended heredity: a new understanding of inheritance and
856 evolution | Princeton University Press Available at:

- 857 <https://press.princeton.edu/books/hardcover/9780691157672/extended-heredity>
858 (Accessed March 10, 2025).
- 859 Buckley, B. A.*, Burkhart, K. B.*, Gu, S. G., Spracklin, G., Kershner, A., Fritz, H., et al. (2012). A
860 nuclear Argonaute promotes multigenerational epigenetic inheritance and germline
861 immortality. *Nature* 489, 447–451. doi: 10.1038/nature11352
- 862 Chen, B., Gilbert, L. A., Cimini, B. A., Schnitzbauer, J., Zhang, W., Li, G.-W., et al. (2013).
863 Dynamic imaging of genomic loci in living human cells by an optimized CRISPR/Cas
864 system. *Cell* 155, 1479–1491. doi: 10.1016/j.cell.2013.12.001
- 865 Chen, S., and Phillips, C. M. (2024). HRDE-2 drives small RNA specificity for the nuclear
866 Argonaute protein HRDE-1. *Nat. Commun.* 15, 957. doi: 10.1038/s41467-024-45245-8
- 867 Chen, X.*, Wang, K.*, Mufti, F. U. D.*, Xu, D., Zhu, C., Huang, X., et al. (2024). Germ granule
868 compartments coordinate specialized small RNA production. *Nat. Commun.* 15, 5799.
869 doi: 10.1038/s41467-024-50027-3
- 870 Chou, H. T., Valencia, F., Alexander, J. C., Bell, A. D., Deb, D., Pollard, D. A., et al. (2024).
871 Diversification of small RNA pathways underlies germline RNA interference
872 incompetence in wild *Caenorhabditis elegans* strains. *Genetics* 226, iyad191. doi:
873 10.1093/genetics/iyad191
- 874 Coffman, S. R., Lu, J., Guo, X., Zhong, J., Jiang, H., Broitman-Maduro, G., et al. (2017).
875 *Caenorhabditis elegans* RIG-I homolog mediates antiviral RNA interference
876 downstream of Dicer-dependent biogenesis of viral small interfering RNAs. *mBio* 8,
877 10.1128/mbio.00264-17. doi: 10.1128/mbio.00264-17
- 878 Consalvo, C. D., Aderounmu, A. M.*, Donelick, H. M.*, Aruscavage, P. J., Eckert, D. M., Shen,
879 P. S., et al. (2024). *Caenorhabditis elegans* Dicer acts with the RIG-I-like helicase DRH-
880 1 and RDE-4 to cleave dsRNA. *eLife* 13, RP93979. doi: 10.7554/eLife.93979
- 881 Cook, D. E., Zdraljevic, S., Roberts, J. P., and Andersen, E. C. (2017). CeNDR, the
882 *Caenorhabditis elegans* natural diversity resource. *Nucleic Acids Res.* 45, D650–D657.
883 doi: 10.1093/nar/gkw893
- 884 Crombie, T. A., Zdraljevic, S., Cook, D. E., Tanny, R. E., Brady, S. C., Wang, Y., et al. (2019).
885 Deep sampling of Hawaiian *Caenorhabditis elegans* reveals high genetic diversity and
886 admixture with global populations. *eLife* 8, e50465. doi: 10.7554/eLife.50465
- 887 Cubas, P., Vincent, C., and Coen, E. (1999). An epigenetic mutation responsible for natural
888 variation in floral symmetry. *Nature* 401, 157–161. doi: 10.1038/43657
- 889 Day, T.#, and Bonduriansky, R. (2011). A unified approach to the evolutionary consequences
890 of genetic and nongenetic inheritance. *Am. Nat.* 178, E18–E36. doi: 10.1086/660911
- 891 de Vanssay, A., Bougé, A.-L., Boivin, A., Hermant, C., Teyssset, L., Delmarre, V., et al. (2012).
892 Paramutation in *Drosophila* linked to emergence of a piRNA-producing locus. *Nature*
893 490, 112–115. doi: 10.1038/nature11416

- 894 Dey, S., Proulx, S. R.#, and Teotónio, H.# (2016). Adaptation to temporally fluctuating
895 environments by the evolution of maternal effects. *PLoS Biol.* 14, e1002388. doi:
896 10.1371/journal.pbio.1002388
- 897 Dirksen, P., Marsh, S. A., Braker, I., Heitland, N., Wagner, S., Nakad, R., et al. (2016). The
898 native microbiome of the nematode *Caenorhabditis elegans*: gateway to a new host-
899 microbiome model. *BMC Biol.* 14, 38. doi: 10.1186/s12915-016-0258-1
- 900 Du, Z.*, Shi, K.*, Brown, J. S., He, T., Wu, W.-S., Zhang, Y., et al. (2023). Condensate
901 cooperativity underlies transgenerational gene silencing. *Cell Rep.* 42, 112859. doi:
902 10.1016/j.celrep.2023.112859
- 903 Duchaine, T. F., Wohlschlegel, J. A., Kennedy, S., Bei, Y., Conte, D., Pang, K., et al. (2006).
904 Functional proteomics reveals the biochemical niche of *C. elegans* DCR-1 in multiple
905 small-RNA-mediated pathways. *Cell* 124, 343–354. doi: 10.1016/j.cell.2005.11.036
- 906 Duempelmann, L.*, Skribbe, M.*, and Bühler, M. (2020). Small RNAs in the transgenerational
907 inheritance of epigenetic information. *Trends Genet.* 36, 203–214. doi:
908 10.1016/j.tig.2019.12.001
- 909 El Mouridi, S., AlHarbi, S., and Frøkjær-Jensen, C. (2021). A histamine-gated channel is an
910 efficient negative selection marker for *C. elegans* transgenesis. *MicroPublication Biol.*
911 doi: 10.17912/micropub.biology.000349
- 912 El Mouridi, S., Alkhalidi, F., and Frøkjær-Jensen, C. (2022). Modular safe-harbor transgene
913 insertion for targeted single-copy and extrachromosomal array integration in
914 *Caenorhabditis elegans*. *G3 GenesGenomesGenetics* 12, jkac184. doi:
915 10.1093/g3journal/jkac184
- 916 El Mouridi, S., Peng, Y., and Frøkjær-Jensen, C. (2020). Characterizing a strong pan-muscular
917 promoter (*Pmlc-1*) as a fluorescent co-injection marker to select for single-copy
918 insertions. *MicroPublication Biol.* doi: 10.17912/micropub.biology.000302
- 919 Félix, M.-A.#, and Duvéau, F. (2012). Population dynamics and habitat sharing of natural
920 populations of *Caenorhabditis elegans* and *C. briggsae*. *BMC Biol.* 10, 59. doi:
921 10.1186/1741-7007-10-59
- 922 Fischer, S. E. J.*, Butler, M. D.*, Pan, Q., and Ruvkun, G. (2008). Trans-splicing in *C. elegans*
923 generates the negative RNAi regulator ERI-6/7. *Nature* 455, 491–496. doi:
924 10.1038/nature07274
- 925 Fischer, S. E. J., Montgomery, T. A., Zhang, C., Fahlgren, N., Breen, P. C., Hwang, A., et al.
926 (2011). The ERI-6/7 helicase acts at the first stage of an siRNA amplification pathway
927 that targets recent gene duplications. *PLOS Genet.* 7, e1002369. doi:
928 10.1371/journal.pgen.1002369
- 929 Fischer, S. E. J.#, and Ruvkun, G.# (2020). *Caenorhabditis elegans* ADAR editing and the ERI-
930 6/7/MOV10 RNAi pathway silence endogenous viral elements and LTR

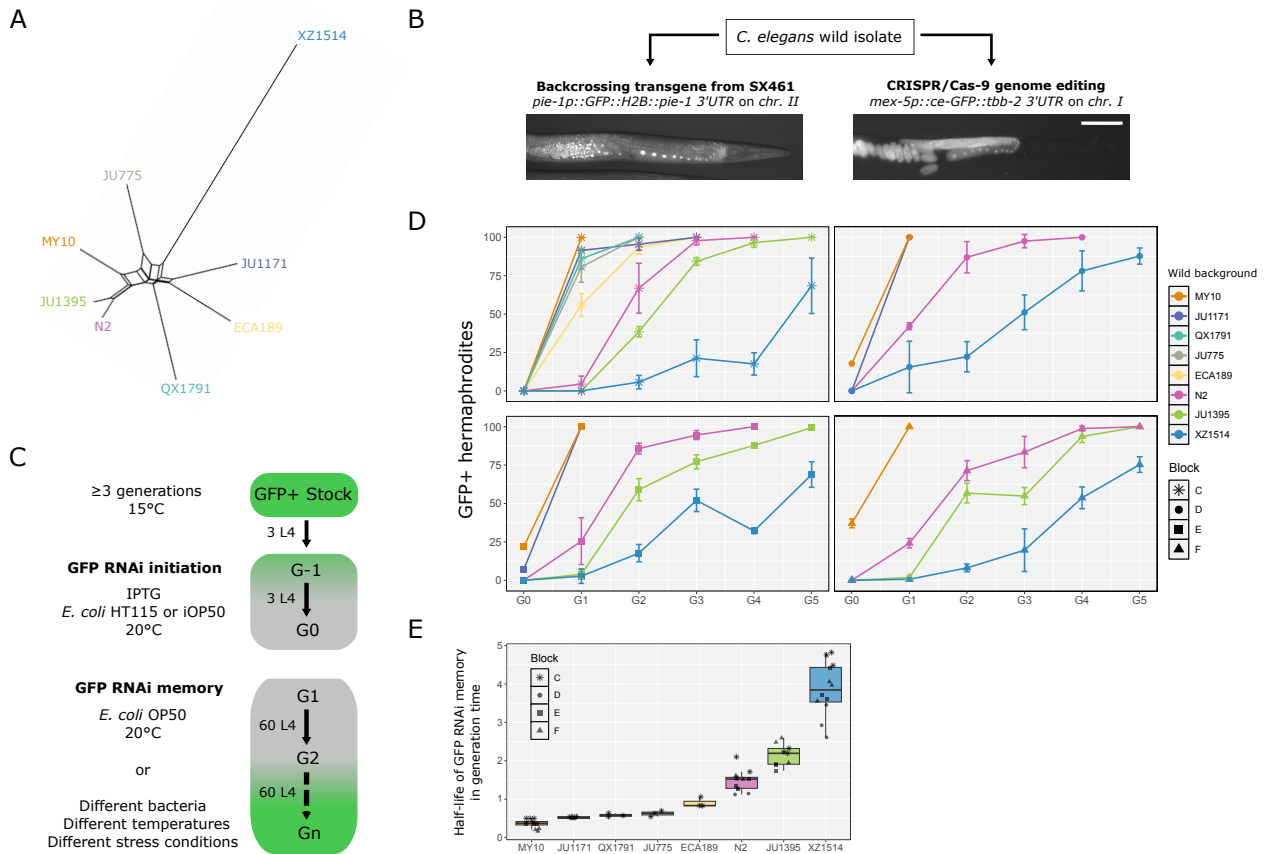
- 931 retrotransposons. *Proc. Natl. Acad. Sci. U. S. A.* 117, 5987–5996. doi:
932 10.1073/pnas.1919028117
- 933 Fitz-James, M. H., and Cavalli, G. (2022). Molecular mechanisms of transgenerational
934 epigenetic inheritance. *Nat. Rev. Genet.* 23, 325–341. doi: 10.1038/s41576-021-
935 00438-5
- 936 Frézal, L., Demoinet, E., Braendle, C., Miska, E.#, and Félix, M.-A.# (2018). Natural genetic
937 variation in a multigenerational phenotype in *C. elegans*. *Curr. Biol.* 28, 2588-2596.e8.
938 doi: 10.1016/j.cub.2018.05.091
- 939 Frézal, L.#, and Félix, M.-A.# (2015). *C. elegans* outside the Petri dish. *eLife* 4, e05849. doi:
940 10.7554/eLife.05849
- 941 Frézal, L.*, Saglio, M.*, Zhang, G., Noble, L., Richaud, A., and Félix, M. (2023). Genome-wide
942 association and environmental suppression of the mortal germline phenotype of wild
943 *C. elegans*. *EMBO Rep.* 24, e58116. doi: 10.15252/embr.202358116
- 944 Frøkjær-Jensen, C., Wayne Davis, M., Hopkins, C. E., Newman, B. J., Thummel, J. M., Olesen,
945 S.-P., et al. (2008). Single-copy insertion of transgenes in *Caenorhabditis elegans*. *Nat.*
946 *Genet.* 40, 1375–1383. doi: 10.1038/ng.248
- 947 Gibson, D. G., Young, L., Chuang, R.-Y., Venter, J. C., Hutchison, C. A., and Smith, H. O. (2009).
948 Enzymatic assembly of DNA molecules up to several hundred kilobases. *Nat. Methods*
949 6, 343–345. doi: 10.1038/nmeth.1318
- 950 González, R.#, and Félix, M.-A.# (2024). Naturally-associated bacteria modulate Orsay virus
951 infection of *Caenorhabditis elegans*. *PLoS Pathog.* 20, e1011947. doi:
952 10.1371/journal.ppat.1011947
- 953 Grishok, A., Tabara, H., and Mello, C. C. (2000). Genetic requirements for inheritance of RNAi
954 in *C. elegans*. *Science* 287, 2494–2497. doi: 10.1126/science.287.5462.2494
- 955 Gu, S. G., Pak, J., Guang, S., Maniar, J. M., Kennedy, S., and Fire, A. (2012). Amplification of
956 siRNA in *Caenorhabditis elegans* generates a transgenerational sequence-targeted
957 histone H3 lysine 9 methylation footprint. *Nat. Genet.* 44, 157–164. doi:
958 10.1038/ng.1039
- 959 Heard, E.#, and Martienssen, R. A.# (2014). Transgenerational epigenetic inheritance: myths
960 and mechanisms. *Cell* 157, 95–109. doi: 10.1016/j.cell.2014.02.045
- 961 Helanterä, H.#, and Uller, T. (2010). The Price Equation and Extended Inheritance. *Philos.*
962 *Theory Biol.* 2. doi: 10.3998/ptb.6959004.0002.001
- 963 Hibshman, J. D*., Webster, A. K*., and Baugh, L. R. (2021). Liquid-culture protocols for
964 synchronous starvation, growth, dauer formation, and dietary restriction of
965 *Caenorhabditis elegans*. *STAR Protoc.* 2, 100276. doi: 10.1016/j.xpro.2020.100276

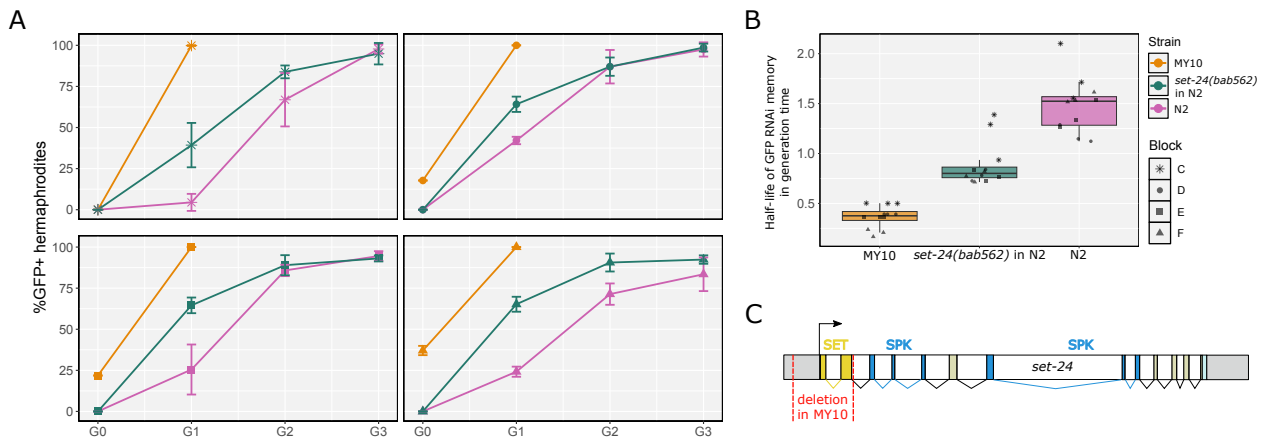
- 966 Hodgkin, J.#, Félix, M.-A., Clark, L. C., Stroud, D., and Gravato-Nobre, M. J. (2013). Two
967 *Leucobacter* strains exert complementary virulence on *Caenorhabditis* including
968 death by worm-star formation. *Curr. Biol.* 23, 2157–2161. doi:
969 10.1016/j.cub.2013.08.060
- 970 Hourí-Zeevi, L.#, Korem Kohanim, Y., Antonova, O., and Rechavi, O.# (2020). Three rules
971 explain transgenerational small RNA inheritance in *C. elegans*. *Cell* 182, 1186-
972 1197.e12. doi: 10.1016/j.cell.2020.07.022
- 973 Hourí-Ze'evi, L., Korem, Y., Sheftel, H., Faigenbloom, L., Toker, I. A., Dagan, Y., et al. (2016). A
974 tunable mechanism determines the duration of the transgenerational small RNA
975 inheritance in *C. elegans*. *Cell* 165, 88–99. doi: 10.1016/j.cell.2016.02.057
- 976 Hourí-Zeevi, L.#, Teichman, G., Gingold, H., and Rechavi, O.# (2021). Stress resets ancestral
977 heritable small RNA responses. *eLife* 10, e65797. doi: 10.7554/eLife.65797
- 978 Hu, P. J. (2007). Dauer. *WormBook Online Rev. C elegans Biol.*, 1–19. doi:
979 10.1895/wormbook.1.144.1
- 980 Huson, D. H., and Bryant, D. (2006). Application of phylogenetic networks in evolutionary
981 studies. *Mol. Biol. Evol.* 23, 254–267. doi: 10.1093/molbev/msj030
- 982 Jablonka, E., Oborny, B., Molnár, I., Kisdi, E., Hofbauer, J., and Czárán, T. (1995). The adaptive
983 advantage of phenotypic memory in changing environments. *Philos. Trans. R. Soc.*
984 *Lond. B. Biol. Sci.* 350, 133–141. doi: 10.1098/rstb.1995.0147
- 985 Karin, O.#, Miska, E. A., and Simons, B. D.# (2023). Epigenetic inheritance of gene silencing is
986 maintained by a self-tuning mechanism based on resource competition. *Cell Syst.* 14,
987 24-40.e11. doi: 10.1016/j.cels.2022.12.003
- 988 Karp, X. (2018). Working with dauer larvae. *WormBook Online Rev. C. elegans Biol.* 2018, 1–
989 19. doi: 10.1895/wormbook.1.180.1
- 990 Kennedy, S., Wang, D., and Ruvkun, G. (2004). A conserved siRNA-degrading RNase
991 negatively regulates RNA interference in *C. elegans*. *Nature* 427, 645–649. doi:
992 10.1038/nature02302
- 993 Klosin, A., Casas, E., Hidalgo-Carcedo, C., Vavouri, T.#, and Lehner, B.# (2017).
994 Transgenerational transmission of environmental information in *C. elegans*. *Science*
995 356, 320–323. doi: 10.1126/science.aah6412
- 996 Knudsen-Palmer, D. R., Raman, P., Etefa, F., De Ravin, L., and Jose, A. M. (2024). Target-
997 specific requirements for RNA interference can arise through restricted RNA
998 amplification despite the lack of specialized pathways. *eLife* 13, RP97487. doi:
999 10.7554/eLife.97487
- 1000 Lachmann, M., and Jablonka, E. (1996). The inheritance of phenotypes: an adaptation to
1001 fluctuating environments. *J. Theor. Biol.* 181, 1–9. doi: 10.1006/jtbi.1996.0109

- 1002 Lee, R. C., Hammell, C. M., and Ambros, V. (2006). Interacting endogenous and exogenous
1003 RNAi pathways in *Caenorhabditis elegans*. *RNA* 12, 589–597. doi:
1004 10.1261/rna.2231506
- 1005 Lev, I.*, Seroussi, U.*, Gingold, H., Bril, R., Anava, S., and Rechavi, O. (2017). MET-2-
1006 dependent H3K9 methylation suppresses transgenerational small RNA inheritance.
1007 *Curr. Biol.* 27, 1138–1147. doi: 10.1016/j.cub.2017.03.008
- 1008 Lind, M. I.*#, and Spagopoulou, F.*# (2018). Evolutionary consequences of epigenetic
1009 inheritance. *Heredity* 121, 205–209. doi: 10.1038/s41437-018-0113-y
- 1010 Mao, K., Breen, P., and Ruvkun, G. (2020). Mitochondrial dysfunction induces RNA
1011 interference in *C. elegans* through a pathway homologous to the mammalian RIG-I
1012 antiviral response. *PLOS Biol.* 18, e3000996. doi: 10.1371/journal.pbio.3000996
- 1013 Mello, C. C., Kramer, J. M., Stinchcomb, D., and Ambros, V. (1991). Efficient gene transfer in
1014 *C. elegans*: extrachromosomal maintenance and integration of transforming
1015 sequences. *EMBO J.* 10, 3959–3970. doi: 10.1002/j.1460-2075.1991.tb04966.x
- 1016 Merritt, C., Rasoloson, D., Ko, D., and Seydoux, G. (2008). 3' UTRs are the primary regulators
1017 of gene expression in the *C. elegans* germline. *Curr. Biol.* 18, 1476–1482. doi:
1018 10.1016/j.cub.2008.08.013
- 1019 Miska, E. A., and Ferguson-Smith, A. C. (2016). Transgenerational inheritance: models and
1020 mechanisms of non-DNA sequence-based inheritance. *Science* 354, 59–63. doi:
1021 10.1126/science.aaf4945
- 1022 Ortiz, E. M. (2019). vcf2phyloip v2.0: convert a VCF matrix into several matrix formats for
1023 phylogenetic analysis. doi: 10.5281/zenodo.2540861
- 1024 Ouyang, J. P. T., Zhang, W. L., and Seydoux, G. (2022). The conserved helicase ZNFX-1
1025 memorializes silenced RNAs in perinuclear condensates. *Nat. Cell Biol.* 24, 1129–
1026 1140. doi: 10.1038/s41556-022-00940-w
- 1027 Paaby, A. B.#, White, A. G., Riccardi, D. D., Gunsalus, K. C., Piano, F., and Rockman, M. V.#
1028 (2015). Wild worm embryogenesis harbors ubiquitous polygenic modifier variation.
1029 *eLife* 4, e09178. doi: 10.7554/eLife.09178
- 1030 Pak, J., and Fire, A. (2007). Distinct Populations of Primary and Secondary Effectors During
1031 RNAi in *C. elegans*. *Science* 315, 241–244. doi: 10.1126/science.1132839
- 1032 Pak, J., Maniar, J. M., Mello, C. C., and Fire, A. (2012). Protection from Feed-Forward
1033 Amplification in an Amplified RNAi Mechanism. *Cell* 151, 885–899. doi:
1034 10.1016/j.cell.2012.10.022
- 1035 Pollard, D. A., and Rockman, M. V. (2013). Resistance to germline RNA interference in a
1036 *Caenorhabditis elegans* wild isolate exhibits complexity and nonadditivity. *G3*
1037 *Bethesda Md* 3, 941–947. doi: 10.1534/g3.113.005785

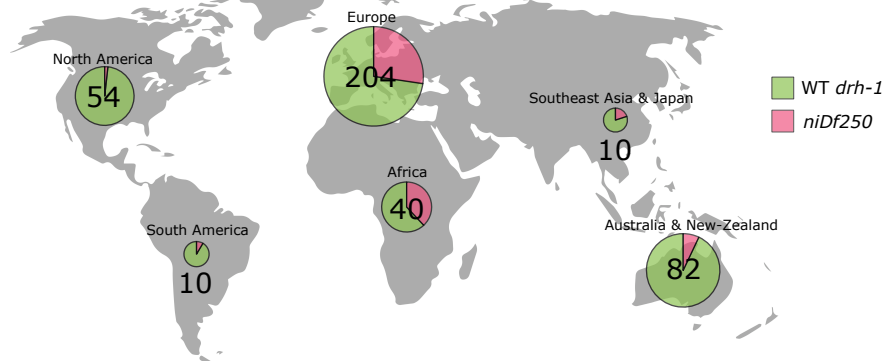
- 1038 Radman, I., Greiss, S.#, and Chin, J. W.# (2013). Efficient and rapid *C. elegans* transgenesis by
1039 bombardment and hygromycin B selection. *PLOS ONE* 8, e76019. doi:
1040 10.1371/journal.pone.0076019
- 1041 Rivoire, O., and Leibler, S. (2014). A model for the generation and transmission of variations
1042 in evolution. *Proc. Natl. Acad. Sci. U. S. A.* 111, E1940-1949. doi:
1043 10.1073/pnas.1323901111
- 1044 Samuel, B. S., Rowedder, H., Braendle, C., Félix, M.-A.#, and Ruvkun, G.# (2016).
1045 *Caenorhabditis elegans* responses to bacteria from its natural habitats. *Proc. Natl.*
1046 *Acad. Sci.* 113, E3941–E3949. doi: 10.1073/pnas.1607183113
- 1047 Schott, D.#, Yanai, I., and Hunter, C. P.# (2014). Natural RNA interference directs a heritable
1048 response to the environment. *Sci. Rep.* 4, 7387. doi: 10.1038/srep07387
- 1049 Schulenburg, H.#, and Félix, M.-A.# (2017). The natural biotic environment of *Caenorhabditis*
1050 *elegans*. *Genetics* 206, 55–86. doi: 10.1534/genetics.116.195511
- 1051 Shukla, A., Perales, R., and Kennedy, S. (2021). piRNAs coordinate poly(UG) tailing to prevent
1052 aberrant and perpetual gene silencing. *Curr. Biol.* 31, 4473-4485.e3. doi:
1053 10.1016/j.cub.2021.07.076
- 1054 Sijen, T.*, Fleenor, J.*, Simmer, F.*, Thijssen, K. L., Parrish, S., Timmons, L., et al. (2001). On
1055 the Role of RNA Amplification in dsRNA-Triggered Gene Silencing. *Cell* 107, 465–476.
1056 doi: 10.1016/S0092-8674(01)00576-1
- 1057 Sowa, J. N., Jiang, H., Somasundaram, L., Tecle, E., Xu, G., Wang, D., et al. (2020). The
1058 *Caenorhabditis elegans* RIG-I homolog DRH-1 mediates the intracellular pathogen
1059 response upon viral infection. *J. Virol.* 94, 10.1128/jvi.01173-19. doi:
1060 10.1128/jvi.01173-19
- 1061 Spracklin, G., Fields, B., Wan, G., Becker, D., Wallig, A., Shukla, A., et al. (2017). The RNAi
1062 inheritance machinery of *Caenorhabditis elegans*. *Genetics* 206, 1403–1416. doi:
1063 10.1534/genetics.116.198812
- 1064 Stiernagle, T. (2006). Maintenance of *C. elegans*. *WormBook Online Rev. C elegans Biol.*, 1–
1065 11. doi: 10.1895/wormbook.1.101.1
- 1066 Sturm, Á.*, Saskó, É.*, Tibor, K., Weinhardt, N., and Vellai, T. (2018). Highly efficient RNAi
1067 and Cas9-based auto-cloning systems for *C. elegans* research. *Nucleic Acids Res.* 46,
1068 e105. doi: 10.1093/nar/gky516
- 1069 Tabara, H., Yigit, E., Siomi, H., and Mello, C. C. (2002). The dsRNA binding protein RDE-4
1070 interacts with RDE-1, DCR-1, and a DExH-Box Helicase to Direct RNAi in *C. elegans*.
1071 *Cell* 109, 861–871. doi: 10.1016/S0092-8674(02)00793-6
- 1072 Timmons, L., Court, D. L., and Fire, A. (2001). Ingestion of bacterially expressed dsRNAs can
1073 produce specific and potent genetic interference in *Caenorhabditis elegans*. *Gene*
1074 263, 103–112. doi: 10.1016/S0378-1119(00)00579-5

- 1075 Tsai, H.-Y., Chen, C.-C. G., Conte, D., Moresco, J. J., Chaves, D. A., Mitani, S., et al. (2015). A
1076 Ribonuclease Coordinates siRNA Amplification and mRNA Cleavage during RNAi. *Cell*
1077 160, 407–419. doi: 10.1016/j.cell.2015.01.010
- 1078 Vasale, J. J.*, Gu, W.*, Thivierge, C., Batista, P. J., Claycomb, J. M., Youngman, E. M., et al.
1079 (2010). Sequential rounds of RNA-dependent RNA transcription drive endogenous
1080 small-RNA biogenesis in the ERGO-1/Argonaute pathway. *Proc. Natl. Acad. Sci.* 107,
1081 3582–3587. doi: 10.1073/pnas.0911908107
- 1082 Vastenhouw, N. L., Brunschwig, K., Okihara, K. L., Müller, F., Tijsterman, M., and Plasterk, R.
1083 H. A. (2006). Gene expression: long-term gene silencing by RNAi. *Nature* 442, 882.
1084 doi: 10.1038/442882a
- 1085 Weigel, D.#, and Colot, V.# (2012). Epialleles in plant evolution. *Genome Biol.* 13, 249. doi:
1086 10.1186/gb-2012-13-10-249
- 1087 Woodhouse, R. M., Buchmann, G., Hoe, M., Harney, D. J., Low, J. K. K., Larance, M., et al.
1088 (2018). Chromatin modifiers SET-25 and SET-32 are required for establishment but
1089 not long-term maintenance of transgenerational epigenetic inheritance. *Cell Rep.* 25,
1090 2259-2272.e5. doi: 10.1016/j.celrep.2018.10.085
- 1091 Wu, X., Shi, Z., Cui, M., Han, M., and Ruvkun, G. (2012). Repression of Germline RNAi
1092 Pathways in Somatic Cells by Retinoblastoma Pathway Chromatin Complexes. *PLOS*
1093 *Genet.* 8, e1002542. doi: 10.1371/journal.pgen.1002542
- 1094 Xu, F.*, Feng, X.*, Chen, X., Weng, C., Yan, Q., Xu, T., et al. (2018). A Cytoplasmic Argonaute
1095 Protein Promotes the Inheritance of RNAi. *Cell Rep.* 23, 2482–2494. doi:
1096 10.1016/j.celrep.2018.04.072
- 1097 Zeiser, E., Frøkjær-Jensen, C., Jorgensen, E., and Ahringer, J. (2011). MosSCI and Gateway
1098 compatible plasmid toolkit for constitutive and inducible expression of transgenes in
1099 the *C. elegans* germline. *PLOS ONE* 6, e20082. doi: 10.1371/journal.pone.0020082
- 1100 Zeng, C.*, Furlan, G.*, Almeida, M. V.*, Rueda-Silva, J. C., Price, J., Mars, J., et al. (2025). A
1101 SET domain-containing protein and HCF-1 maintain transgenerational epigenetic
1102 memory. 2025.03.25.645221. doi: 10.1101/2025.03.25.645221
- 1103 Zhang, G.#, Félix, M.-A.#, and Andersen, E. C.# (2024). Transposon-mediated genic
1104 rearrangements underlie variation in small RNA pathways. *Sci. Adv.* 10, eado9461.
1105 doi: 10.1126/sciadv.ado9461
- 1106

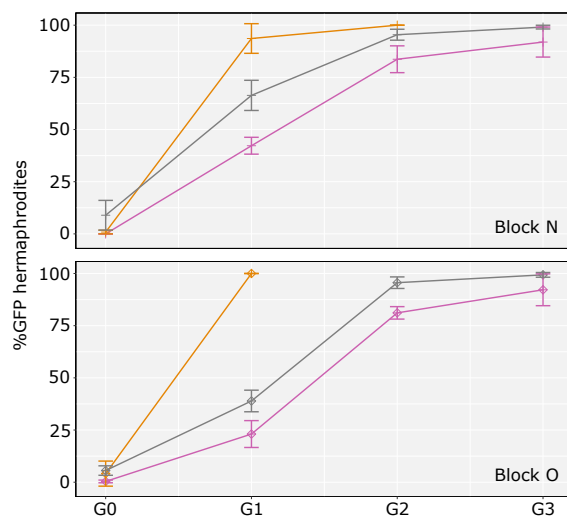




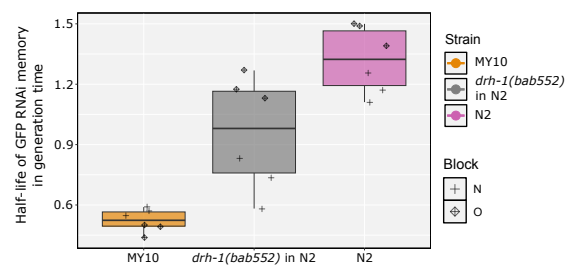
A



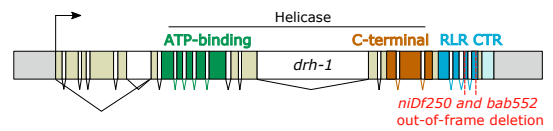
B

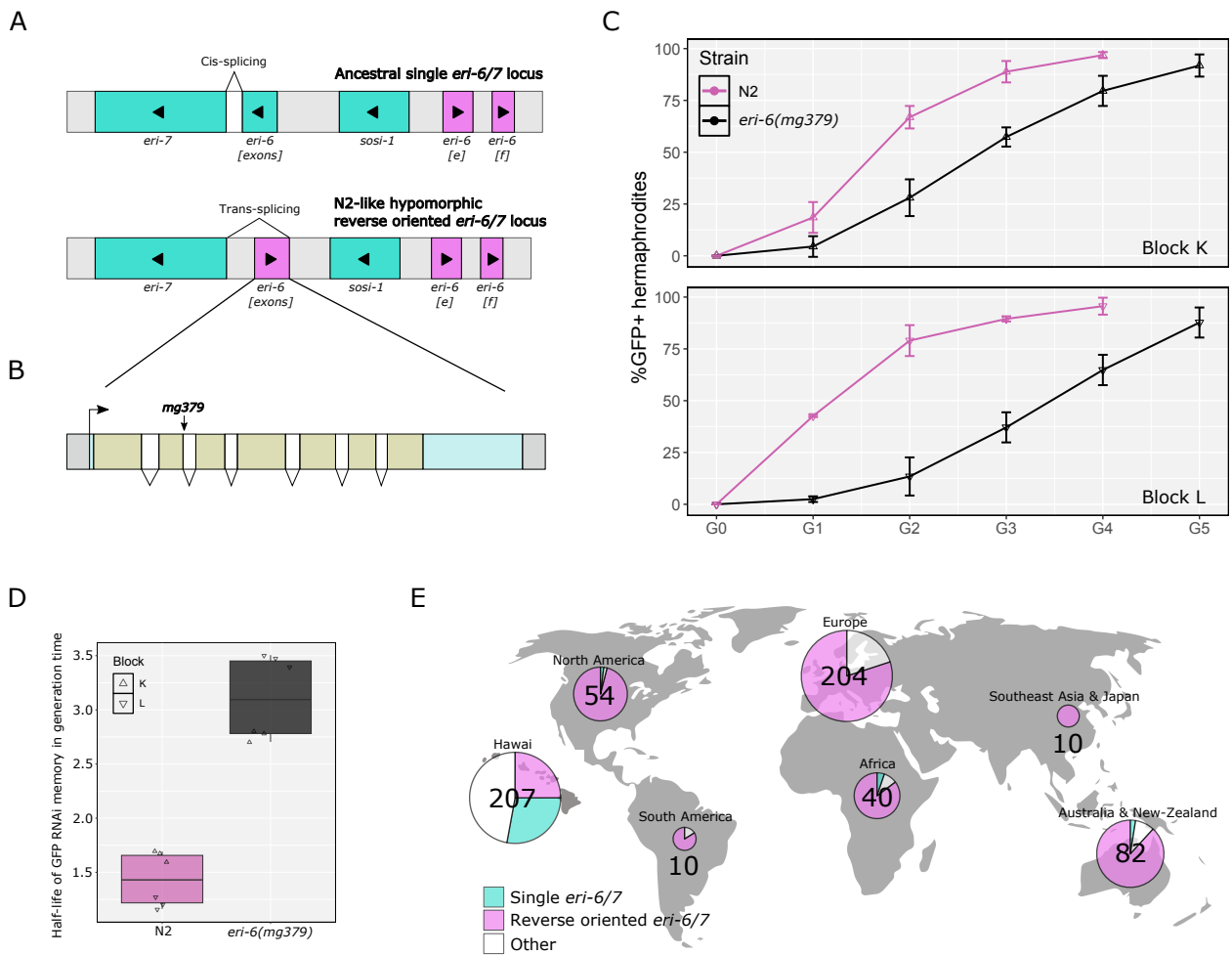


C

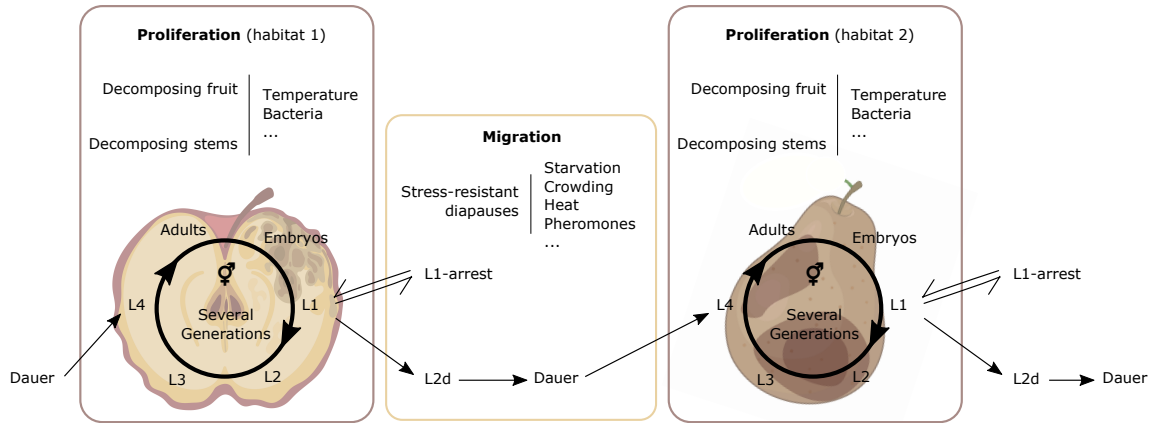


D

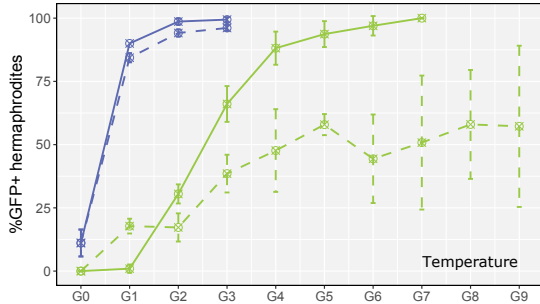




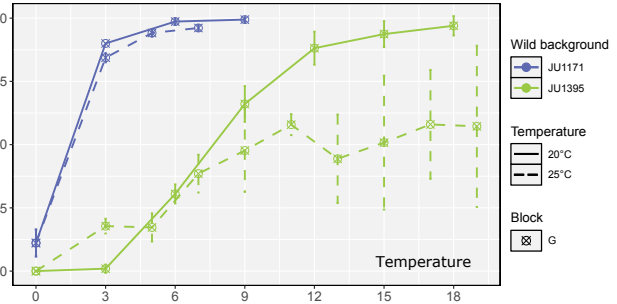
A



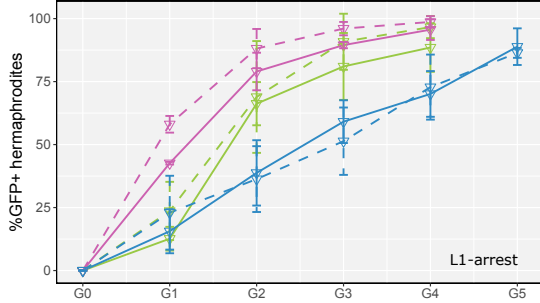
B



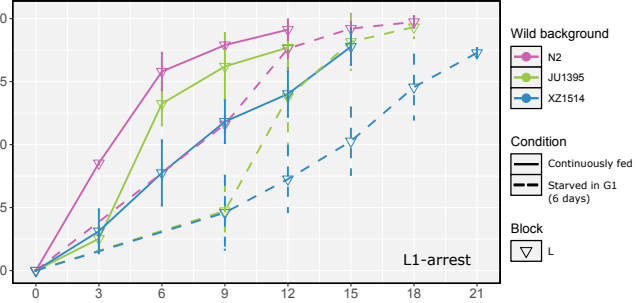
C



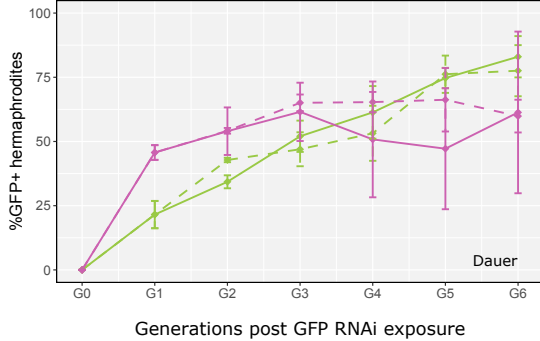
D



E



F



G

